Ann. Geophys., 31, 725–743, 2013
www.ann-geophys.net/31/725/2013/
doi:10.5194/angeo-31-725-2013

Annales Geophysicae
Open Access

Spectral structure of Pc3–4 pulsations: possible signatures of cavity modes

P. R. Sutcliffe[1], **B. Heilig**[2], **and S. Lotz**[1]

[1]South African National Space Agency (SANSA) Space Science, Hermanus, South Africa
[2]Tihany Geophysical Observatory, Geological and Geophysical Institute of Hungary, Tihany, Hungary

Correspondence to: P. R. Sutcliffe (psutcliffe@sansa.org.za)

Received: 12 September 2012 – Revised: 19 March 2013 – Accepted: 20 March 2013 – Published: 23 April 2013

Abstract. In this study we investigate the spectral structure of Pc3–4 pulsations observed at low and midlatitudes. For this purpose, ground-based magnetometer data recorded at the MM100 stations in Europe and at two low latitude stations in South Africa were used. In addition, fluxgate magnetometer data from the CHAMP (CHAllenging Minisatellite Payload) low Earth orbit satellite were used. The results of our analysis suggest that at least three mechanisms contribute to the spectral content of Pc3–4 pulsations typically observed at these latitudes. We confirm that a typical Pc3–4 pulsation contains a field line resonance (FLR) contribution, with latitude dependent frequency, and an upstream wave (UW) contribution, with frequency proportional to the IMF (interplanetary magnetic field) magnitude B_{IMF}. Besides the FLR and UW contributions, the Pc3–4 pulsations consistently contain signals at other frequencies that are independent of latitude and B_{IMF}. We suggest that the most likely explanation for these additional frequency contributions is that they are fast mode resonances (FMRs) related to cavity, waveguide, or virtual modes. Although the above contributions to the pulsation spectral structure have been reported previously, we believe that this is the first time where evidence is presented showing that they are all present simultaneously in both ground-based and satellite data.

Keywords. Magnetospheric physics (Magnetosphere–ionosphere interactions)

1 Introduction

The geomagnetic pulsations most commonly observed at low to middle latitudes during local daytime are Pc3 and Pc4 quasi-sinusoidal continuous pulsations, with periods ranging from 10–150 s. These pulsations are most commonly associated with field line resonances (FLRs) in the plasmasphere (e.g. Waters et al., 1991, 1994; Verõ et al., 1998; Vellante et al., 2004; Ndiitwani and Sutcliffe, 2009). It is also commonly suggested that the energy source which drives the FLRs are upstream waves (UWs) generated in the Earth's foreshock (e.g. Russel and Hoppe, 1981; Yumoto et al., 1984; Takahashi et al., 1984; Engebretson et al., 1986, 1987). Contrarily, a number of investigations using numerical modelling have suggested that cavity or waveguide modes in the magnetosphere are the drivers of the FLRs (Allan et al., 1985; Samson et al., 1995; Waters et al., 2000). A few studies have also presented results in support of the observation of these fast mode resonances (FMRs) in ground-based data (Samson et al., 1995; Menk et al., 2000). However, direct observational evidence for FMRs in satellite data is sparse (Waters et al., 2002). Verõ et al. (1998) investigated the relationship between FLRs and UWs but alluded to the possible presence of signals from another unidentified source.

The objective of this study is to show that Pc3–4 pulsations at low and midlatitudes contain signals arising from at least three different sources or mechanisms. In order to achieve this, we investigate the spectral structure of pulsations observed at low and midlatitudes in an attempt to clarify their make-up. In particular, we wish to show that Pc3–4 pulsations comprise an UW contribution, FLR harmonics, plus other structure, which is most likely due to cavity, waveguide, or virtual modes. We show that each of these contributions can be isolated in the spectra of pulsation signals observed on the ground and at low Earth orbit satellite altitudes. Although the above contributions to Pc3–4 pulsation structure have all been reported previously, we believe that this is the first time where evidence is presented showing that

they are all present simultaneously in both ground-based and satellite data.

Since the earliest observations of the near-Earth solar wind in the 1960s and 1970s, the possibility of extra-magnetospheric sources of pulsation activity had been proposed, due to the correlation between solar wind parameters and pulsation observations. Troitskaya (1994) reviews much of the work by Soviet scientists conducted during this period. Particularly, power in the Pc3–4 band increases with solar wind speed (Saito, 1964) and the frequency of pulsations observed on the Earth's surface is linearly related to the magnitude of the interplanetary magnetic field (IMF) (Bol'shakova and Troitskaya, 1968; Troitskaya et al., 1971). Later, Russell and Hoppe (1981) showed that the linear relationship between IMF magnitude and pulsation frequency also holds between IMF magnitude and the frequency of the upstream waves, suggesting that UWs act as a source of Pc3s in the magnetosphere. The linear relationship between frequency and field magnitude suggests that waves are generated by cyclotron motion of charged particles around magnetic field lines. Fairfield (1969) first reported observations of low frequency waves (10–50 mHz) in the region upstream of the bow shock and noted that waves are only observed on field lines that intersect the bow shock. Barnes (1970) and Gary (1991) explained that these waves may be generated by an ion-cyclotron instability set up due the solar wind counter-streaming with ions reflected upstream off the bow shock. The upstream propagating waves are convected downstream by the solar wind and converted from fairly monochromatic to lower frequency waves that steepen into shocklets near the bow shock (Le and Russell, 1992). UWs propagate into the magnetosphere when the IMF orientation (quantified by the cone angle θ_{xB} between the sun–Earth line and the IMF direction) is nearly parallel to the sun–Earth line (e.g. Yumoto et al., 1984; Le and Russell, 1992). Engebretson et al. (1986) noted the IMF control of Pc3–4 pulsations when activity at low L shells ($L \sim 3$) suddenly resumed upon IMF orientation changing from quasi-perpendicular (large cone angle) to quasi-parallel (small cone angle). Heilig et al. (2010) showed that the intensity of UW-related Pc3s is dependent on the density of the solar wind, and density-related parameters like the dynamic pressure and distance from the magnetopause to the Earth. A pause in Pc3 activity was observed while the bulk density of protons in the upstream solar wind was extremely low. After the low density anomaly (LDA) the proton density returned to normal and pulsation activity resumed. The dependence of Pc3 activity on solar wind density suggests that UWs are the predominant source of midlatitude Pc3s. A multi-instrument study by Clausen et al. (2009) clearly illustrates the transfer of ULF energy from an upstream source. Simultaneous observations made aboard spacecraft in the solar wind (Geotail) and in the magnetosphere (Cluster), and by magnetometers on the ground showed (i) the excitation of ULF waves in the magnetometers 10 min after the IMF direction changed to a parallel orientation, and (ii) a broad, unstructured band of frequencies in the poloidal and compressional field components, driving multiple harmonics of FLRs in the toroidal field component.

FLR-related pulsations observed at low L values require that waves be sustained to propagate several R_E to the inner magnetosphere where coupling to field line resonances occur. Yumoto (1985) used ISEE 3 (International Sun/Earth Explorer) and GOES 2 (Geostationary Operational Environmental Satellites) observations and measurements from two ground stations to relate solar wind data to Pc3s on the ground and suggested that compressional waves from a broadband source near the magnetopause couples to FLRs near the Earth. Engebretson et al. (1986) cited the same mechanism to explain simultaneous observations of multiple harmonics of toroidal mode FLR's and an increase in broadband compressional wave power. Heilig et al. (2007) computed the latitudinal distribution of dayside Pc3 amplitudes and concluded that UWs enter near the subsolar point as compressional waves where they couple to the Alfvén mode resulting in field line oscillations. High latitude pulsations did not show the same dependence on solar wind parameters (V_{sw}, θ_{xB}, B_{IMF}) as low latitude Pc3s did, possibly indicating different generation mechanisms for high and low/middle latitude pulsations.

Since its launch, observations from the low Earth orbiting CHAMP (CHAllenging Minisatellite Payload) spacecraft, in conjunction with ground based measurements, have been used to directly test the theory of FLR excitation. In similar investigations Vellante et al. (2004) and Ndiitwani and Sutcliffe (2009) observed narrow band compressional wave activity aboard CHAMP coinciding with Pc3 activity on the ground. The fast mode wave frequency structure matches the toroidal component observed by CHAMP, which in turn matches FLR frequencies in the horizontal (H) field component, suggesting FLR excitation by compressional waves. This suggests that narrow and broad bandwidth activity matching the field line eigenfrequencies set up resonances to drive Pc3s (Engebretson et al., 1986). The simultaneous observation of driving (compressional), forced (toroidal) and resultant (H, D component of ground field) oscillations in the generation of a Pc3 pulsation was demonstrated by Ndiitwani and Sutcliffe (2009). Recently Ndiitwani and Sutcliffe (2010) described events with FLRs excited by broadband compressional wave activity. Standing Alfvén waves in the toroidal mode was observed simultaneously with Pc3s on the ground, at a middle latitude station pair ($L \sim 1.8$). Vellante et al. (2004) showed for the first time (and this was confirmed by Ndiitwani and Sutcliffe, 2009) observations demonstrating the 90° rotation of polarisation by the ionosphere. At field line footpoints in the ionosphere the standing waves excited by the FLR are rotated by the ionospheric Hall currents so that they are observed in the H component on the ground (Vellante et al., 2004). The observed rotation by 90° might be regarded as exceptional since it is only expected to occur for a uniform distribution

of ionospheric conductivity; the assumption of uniform ionospheric conductivity distribution is not realistic in general and arbitrary rotation is expected (Glassmeier, 1984). Vellante et al. (2004), Ndiitwani and Sutcliffe (2009), and more recently Heilig et al. (2013) demonstrated the apparent shift in frequency of the shear Alfvén wave component of the pulsations due to rapid motion of CHAMP with respect to the ground stations.

Waters et al. (1991) introduced the cross-phase method to identify field line resonant frequencies from phase spectra from a pair of meridional ground stations. The phase difference is computed and the frequency corresponding to the maximum phase difference is identified as the resonant frequency. Waters et al. (1994) used the cross-phase method to study the temporal behaviour of the resonant structure at two latitudes ($L = 1.8$ and $L = 2.8$). Multiple harmonics are exhibited at the higher latitude station pair, whereas a single frequency is observed at the low latitude station pair, indicative of reduced power at higher frequencies in the magnetosphere. An investigation by Verõ et al. (1998) showed alternating observations of pulsations driven by FLRs, and those driven directly by UWs, within short (~ 1 min) intervals. A third component was observed whose period does not depend on IMF magnitude and does not match the FLR frequency. They noted that the third component was observed about four minutes before an active period in the solar wind, relating its cause to the vicinity of disturbed solar wind plasma.

Kivelson and Southwood (1985) first proposed that the magnetospheric cavity or waveguide mode (Samson et al., 1992) may act as a resonator of ULF waves. An analysis by Samson et al. (1995) of power spectra observed at a number of low latitude stations ($L < 3$) revealed the presence of peaks in power at closely separated frequencies, about 3–5 mHz apart. The fine structure was explained as the observation of multiple waveguide mode harmonics by the ground-based magnetometers. An approximate model (based on the Wentzel–Kramers–Brillouin method) of the waveguide mode predicted a similar close separation between peaks in Pc3 power. The model describes a cavity enclosed by the magnetopause, with turning points in the plasmasphere; this type of waveguide mode is further motivated by their observation that the fine structure seen at $L < 3$ latitudes is not present for a high latitude ($L = 6.7$, i.e. beyond the plasmapause) event. Field line resonant Pc3s are also observed at low latitudes, up to a certain low latitude limit ($L \sim 1.4$ in Menk et al., 2000) as power diminishes due to ion mass loading in the ionosphere, where much of the low latitude field lines reside. Menk et al. (2000) investigated low latitude FLRs ($L \sim 1.3$–2) and observed similar peaks in power spectra, separated by 3–5 mHz. A low frequency component (< 40 mHz) exhibiting phase delays between stations was observed. The delay could not be explained by the propagation time of incoming fast mode waves from higher L shells, and it is suggested that waveguide mode waves driving FLRs are responsible for the low frequency oscillation.

The continuous buffeting of the dayside magnetosphere by the incoming solar wind results in the excitation of surface waves on the magnetopause. Pressure enhancements may act as an impulse exerted on the magnetospheric cavity providing the broadband signal that excites cavity/waveguide mode waves. Following enhancements in the solar wind dynamic pressure Eriksson et al. (2006) observed fast mode compressional waves at two frequencies (6.8 and 27 mHz), which were converted to toroidal and poloidal modes at the same frequencies. This was interpreted as two harmonics of the waveguide mode being excited by a pressure pulse on the magnetopause that eventually coupled to FLRs at the same eigenfrequencies of the field lines. Plaschke et al. (2009) investigated the dependence of magnetopause surface oscillations on different solar wind conditions, using THEMIS (Time History of Events and Macroscale Interactions during Substorms) measurements and OMNI data. They proposed that oscillations of the magnetopause are due to Alfvén waves on the magnetopause surface that develop into standing Alfvén waves, reflecting at field line footpoints in the ionosphere. The magnetopause was found to preferentially oscillate during intervals of northward and quasi-parallel IMF and low solar wind speed.

Recently, Stephenson and Walker (2010) gave evidence of ULF oscillations at 2.1 mHz (in the Pc5 band) originating in the upstream solar wind, which excite compressional waveguide modes in the outer magnetosphere and which, in turn, set up FLRs in near earth space, beyond the waveguide reflection point. Using ACE (Advanced Composition Explorer) and Wind spacecraft measurements of solar wind plasma and magnetic field parameters, and HF radar (SuperDARN, Super Dual Auroral Radar Network) observations to measure FLR activity at a high latitude station (SANAE (South African National Antarctic Expedition), Antarctica) they found high coherence between the amplitude and phase of the two (SW and FLR) signals. Although the study by Stephenson and Walker (2010) concerns Pc5s at high latitude, ULF oscillations in the solar wind directly driving magnetospheric ULF activity is an interesting possibility and must be kept in mind when studying other bands of continuous pulsation.

2 Data selection and analysis

In this study we use spectral analysis techniques to show that Pc3–4 pulsations observed at low and midlatitude ground stations and at F region satellite altitudes contain signals arising from at least three different sources. In particular, we show that besides an UW component and FLR harmonics, Pc3–4 pulsations also contain other structure, which is most likely due to cavity, waveguide or virtual modes. To achieve this, it is necessary to clearly isolate each of these constituents in the spectra of pulsation signals observed on the ground and at low Earth orbit. Since the methodology to identify cavity,

Table 1. Geographic and altitude adjusted corrected geomagnetic coordinates for 2004, 100 km reference height, for stations used in this study.

Station	Geographic coordinates		AACGM coordinates		L shell
	Latitude	Longitude	Latitude	Longitude	
THY	46.90° N	17.89° E	42.41°	92.33°	1.83
NCK	47.63° N	16.72° E	43.24°	91.46°	1.88
BEL	51.83° N	20.80° E	48.01°	96.07°	2.23
TAR	58.26° N	26.46° E	54.85°	102.93°	3.02
NUR	60.52° N	24.65° E	57.26°	102.21°	3.42
HAN	62.30° N	26.65° E	59.04°	104.64°	3.78
SOD	67.37° N	26.63° E	64.20°	107.26°	5.28
KIL	69.02° N	20.79° E	66.14°	103.75°	6.11
SUT	32.40° S	20.67° E	−41.31°	85.32°	1.77
HER	34.43° S	19.22° E	−42.64°	82.89°	1.85

waveguide or virtual modes in pulsation signals is not well established, we place significant emphasis on the identification of the UW and FLR components in order to isolate the third component.

The ground-based observations used consisted of fluxgate magnetometer data recorded at the MM100 stations in Europe (Heilig et al., 2007) and induction magnetometer data from two low latitude stations in South Africa (see Table 1 for the station coordinates). The Hermanus station (HER) in South Africa is roughly conjugate to the lowest latitude MM100 station Tihany (THY) in Hungary. The induction magnetometer data were converted to nT units by correcting for the frequency dependent amplitude and phase response of the system. In addition, fluxgate magnetometer data from the CHAMP low Earth orbit (LEO) satellite (Reigber et al., 2002), which had a near polar circular orbit, were used. The magnetic field measurements from CHAMP are of unprecedented accuracy and resolution, which has enabled clearly resolved observations of Pc3–4 pulsations (Vellante et al., 2004; Heilig et al., 2007; Ndiitwani and Sutcliffe, 2009, 2010). An advantage of CHAMP data over ground-based data for pulsation studies is the ability to easily discriminate between shear Alfvén and fast mode waves. Data selection for this study was made for times when CHAMP was traversing ground-based stations in South Africa or the MM100 stations in Europe. All data were sampled at 1 s intervals and filtered in the Pc3–4 frequency band, i.e. 6.7–100 mHz. Various Fourier auto- and cross-spectral analysis and maximum entropy spectral analysis (MESA) techniques were then used to analyse the data. The time series were numerically differentiated prior to computation of the spectra in order to reduce their slope. When computing geomagnetic pulsation spectra from filtered data, a peak sometimes appears at the low frequency end of the spectrum, which is not real but rather an artefact of the filtering process. The exact location of the peak may depend on the properties of the filter and the nature of the pulsation signal, which typically has a power-law type background spectrum. Since most of the events used in this study exhibited peaks at the low frequency end of the spectrum, particularly around 20 mHz, we checked these to confirm that the peaks were real. This was done by recomputing the spectra with different filter cut-off frequencies and by plotting spectra of unfiltered data on log-log scales; examples of the latter are shown in some of the figures.

In this study we also utilised certain solar wind parameters such as solar wind speed and IMF magnitude and cone angle. For this purpose, we used the one-minute OMNI high resolution solar wind data, which are provided after being time-shifted to the magnetosphere's bow-shock nose from the original locations of the observations and available on the OMNI website: http://omniweb.gsfc.nasa.gov.

2.1 Ground-based data

In the first part of this study, ground-based data alone were used. In this case, it is not straightforward to discriminate between fast mode and shear Alfvén waves, since both manifest themselves in the H (magnetic north) component, due to the effects of the ionosphere. Consequently, it was necessary to utilise special techniques to separate the UW component and the shear Alfvén FLR harmonics from any other fast mode components in the data. We used two approaches to identify the presence of UWs in the pulsation spectra and thus separate them from other fast mode power; the first relies on the way in which the events studied were selected and the second, used by Heilig et al. (2007), is based on determining the cross power from a meridian chain of stations.

Events were selected for days where the IMF total $\boldsymbol{B}$ field varied significantly, the solar wind velocity was relatively stable, and the average cone angle was sufficiently small to allow the occurrence of significant Pc3–4 activity. Since the frequency of the UW component of Pc3–4 pulsations is dependent on the IMF intensity, one can expect the frequency to vary significantly on days where IMF intensity varied.

The approach used by Heilig et al. (2007) for identifying the UW component supposes that the UW signal is coherent over large areas extending up to thousands of kilometers on the ground (Tanaka et al., 1998), whereas the FLR signal of a particular frequency dominates over a limited latitudinal range. The UW activity and other fast mode power should then become evident by calculating the cross-spectral power from the H component data recorded at a meridional chain of stations spanning a range of geomagnetic latitudes while, at the same time, weakening the latitude dependent FLR contributions. The cross-spectral density (CSD $P^n(\omega)$) of n signals is defined as:

$$P^n(\omega) = \sqrt[n]{\prod_{i=1}^{n} \left| \hat{X}_i(\omega) \right|^2},$$

where $\hat{X}_i(\omega)$ is the Fourier transform of $x_i(t)$ time series, t is the time, and ω is the angular frequency.

Baransky et al. (1985) initially proposed a method for the direct measurement of the eigenfrequency of magnetic field lines using ground-based magnetometer data. They demonstrated that either the difference or ratio of Pc3–4 pulsation amplitude spectra observed at two closely spaced meridional ground stations can be used to determine the eigenfrequency associated with the field lines between the two stations. Waters et al. (1991) proposed a more reliable technique of determining the presence of a field line resonance (FLR) by the use of the cross-phase spectrum. With this method the peak in the cross-phase difference of the H components from two closely spaced stations identifies the resonant frequency. Consequently, we used the cross-phase method to determine the presence of field line resonances.

2.2 CHAMP data

The CHAMP data used for this study were the preprocessed data from the fluxgate vector magnetometer (product identifier CH-ME-2-FGM-FGM). The data were rotated into a field-aligned coordinate system determined from the low pass filtered data. In this coordinate system the compressional component (B_{com}) is aligned with the ambient magnetic field direction (positive north), the toroidal component (B_{tor}) represents the azimuthal perturbation (positive east), and the poloidal component (B_{pol}) lies in the magnetic meridian plane (positive inward). Due to CHAMP's low orbit it traverses the L shell structure of geomagnetic field lines very rapidly. Consequently, when the spectral structure of FLRs is studied, standard spectral analysis techniques, such as those based on the FFT (Fourier transformation), are not suitable. Vellante et al. (2004) and Ndiitwani and Sutcliffe (2009) found that maximum entropy spectral analysis (MESA) produces acceptable results under these circumstances. However, Heilig et al. (2007) found that Fourier and wavelet analysis techniques are suitable for the study of fast mode waves, such as UWs, in CHAMP magnetometer data, since their frequencies are not latitude dependent.

Although theoretical and numerical studies have predicted the existence of cavity/waveguide resonance modes in the magnetosphere, experimental evidence is sparse. Consequently, Waters et al. (2002) investigated experimental methods for the detection of ultralow-frequency cavity modes using spacecraft data. They suggested four methods for the detection of fast mode resonances (FMRs) in satellite data, based on an MHD (magnetohydrodynamic) numerical simulation study, namely:

1. Average the compressional component amplitude spectra as the satellite traverses a region in order to identify any dominant peaks.
2. Look for constant tones with radial (L shell) distance in compressional component dynamic spectra.
3. Observe 90° phase difference between the compressional magnetic and azimuthal electric field data to confirm standing wave structure.
4. If two satellites are closely separated radially, examine the phase difference properties of the compressional components' data to reveal FMR nodal structure.

Using maximum entropy (MESA) and FFT spectral analysis techniques, we used the first two of the above methods to show that signals with quasi-constant frequency often persist in the fast mode components as CHAMP rapidly traverses L shells. Note, however, that these two conditions alone are insufficient to identify the signals as resonances, since they are not able to confirm standing wave structure. Unfortunately, the Waters et al. (2002) methods (3 and 4), which are able to confirm standing wave structure, could not be applied, since they require either dual satellites or a single satellite with magnetic and electric field data, neither of which is applicable in CHAMP's case.

2.3 Statistical reliability and band width of spectral estimates

It is necessary to briefly discuss the trade-off between the statistical reliability and bandwidth of FFT spectral estimates, since this is the key to the difference between some previously published results on cavity modes and the results presented in this paper. The statistical reliability of a spectral estimate can be expressed in terms of a confidence interval where use is made of the chi-square distribution (Otnes and Enochson, 1972). This quantity is determined by the number of degrees of freedom n of a spectral estimate. For an individual FFT spectral estimate, Otnes and Enochson (1972) show that in the case of uncorrelated Gaussian noise the stability of the estimate is that of a chi-square distribution with $n = 2$, which in the words of Tukey (1967) is "horribly unstable." In order to improve stability, raw FFT spectral estimates are

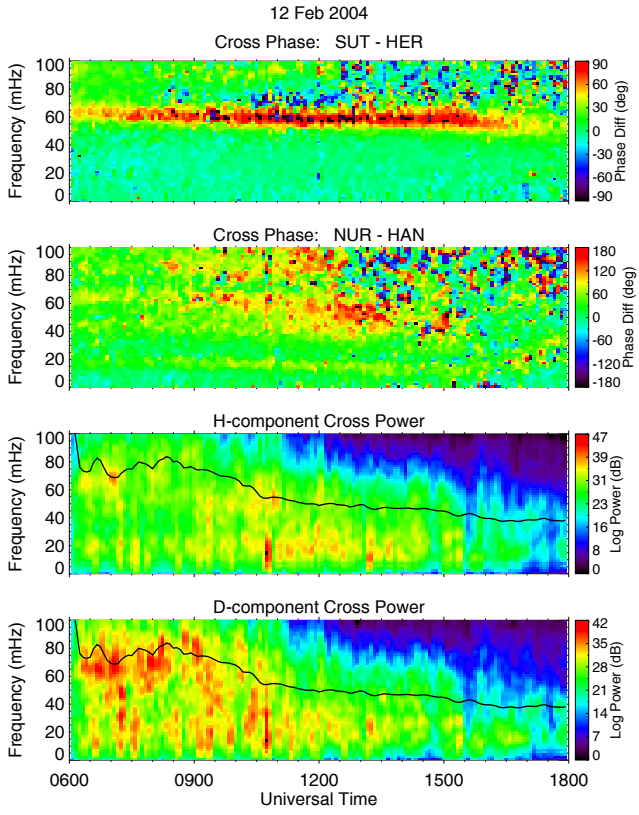

Fig. 1. Dynamic FFT cross phase and power spectra for the Pc3–4 pulsation activity observed during the interval 06:00–18:00 UTC on 12 February 2004. The cross power spectra were computed from all eight of the MM100 stations listed in Table 1.

usually averaged to yield $n = 2M$ where M is the number of contiguous estimates averaged. Most authorities (Tukey, 1967; Bendat and Piersol, 1966; Otnes and Enochson, 1972) advise that at least 10–20 degrees of freedom are required in order to obtain a statistically reliable spectral estimate. For values of n less than this, the variance of the estimates becomes excessive and the spectrum increasingly unstable (Jenkins and Watts, 1968). The bandwidth of an FFT spectral estimate is given by $B = M\Delta f = M/N\Delta t$, where N is the number of data points in the time series and Δt is the sampling interval. The above expressions show that there is of necessity a trade-off between bandwidth and statistical reliability when computing spectral estimates.

When using MESA, the spectral resolution is greatly influenced by the number of terms or order of the prediction error filter (PEF); consequently, it is important to determine and use the correct PEF order (Chen and Stegen, 1974). A PEF order that is too small results in a highly smoothed spectrum where some peaks may not be resolved, thus precluding the advantages of MESA. An excessive PEF order introduces spurious peaks and peak splitting into the spectrum. In Ndiitwani and Sutcliffe's (2009) study of Pc3 pulsations using MESA, the PEF order was established by experimenting with artificially generated signals, consisting of a number of sinusoids and random noise, intended to simulate a Pc3 event. They found that as more random noise was added to the synthetic signal, it was necessary to increase the PEF order to resolve the spectral peaks. A greater PEF order is also required if one of the amplitudes is very much less than the other others. Since the prime objective of Ndiitwani and Sutcliffe's (2009) study was to identify FLRs, which if present, are generally one of the more intense spectral components, they regarded PEF orders of 15 and 20, respectively, for 90 s ground-based and satellite data time series, as adequate. However, they stated that if one were interested in studying the fast mode fine structure in more detail, as is the case for the current study, then a larger PEF order than the above would probably be required.

3 Ground-based observations

3.1 Event of 12 February 2004

The first event considered occurred on 12 February 2004, when the IMF total $\boldsymbol{B}$ field decreased by about 6 nT over a period of 7 h. Figure 1 shows dynamic cross phase and power spectra for the Pc3–4 pulsation activity observed on the ground for the interval 06:00–18:00 UTC (Universal Time Coordinated). The dynamic spectra were computed using an FFT with a 10 min data window, which was progressively shifted by 5 min. The first and last 10 % of data in each data window were tapered by rising and falling cosine bells prior to computing the spectra. Each cross phase (power) spectrum was smoothed using five (nine) spectral estimates averaged under an exponentially tapered window.

The top panel (Fig. 1) shows the phase difference between the low latitude stations SUT and HER; it clearly indicates the occurrence of a field line resonance centered on a frequency of 60 mHz, which decreased slightly through the day. The second panel shows the phase difference between the midlatitude stations NUR and HAN and indicates the occurrence of a field line resonance with harmonic structure. The fundamental frequency decreased from about 20 to 15 mHz through the day. The 3rd and 4th harmonics are the clearest and rather spread in frequency. The lower two panels show the cross power for the H and D components, respectively, computed from all eight of the MM100 stations listed in Table 1. As mentioned previously, the objective of computing the cross power from a meridian chain of stations is that it should accentuate any latitude independent activity, such as UW or other fast mode activity, and suppress the FLR activity. The superimposed black curves on the H and D component panels show how the estimated UW frequency f_{UW} (mHz) $= 6 \cdot B_{\mathrm{IMF}}$ (nT) (Yumoto et al., 1984) varied due to the variation of IMF total field intensity B. The reliability of this estimate was illustrated by Yumoto et al. (1984), who showed that at geosynchronous orbit the frequencies of all Pc3–4

compressional waves considered as functions of B_{IMF} are confined to the region between f (mHz) $= 4.5 \cdot B_{IMF}$ (nT) and f (mHz) $= 7.5 \cdot B_{IMF}$ (nT). The general decrease in UW frequency was due to a decrease in B from about 13 nT around 08:00 UTC to about 7 nT after 15:00 UTC. A broad band of power at the estimated UW frequencies, i.e. which straddles the black curve, is clearly evident, particularly between 06:00 and 13:00 UTC.

The cross power spectra also clearly show oscillations at other frequencies, e.g. there is a broad band of power of variable intensity around 20 mHz and a band of power between 40 and 50 mHz from about 09:00 to 11:00 UTC, which we suggest might be evidence of fast mode resonances (FMR) related to cavity, waveguide or virtual modes. Clearly, these signals are not directly related to UW activity; in particular, the broad 20 mHz signal is evident throughout the day and does not follow the trend of the varying UW frequency. It might be suspected that the signal at 20 mHz is due to FLRs, since this frequency lies close to the fundamental FLR frequency at latitudes around $L = 3$. The MM100 stations are not equally distributed in latitude; consequently, too many stations from this range may over-represent any FLR signals close to 20 mHz in the cross power spectra. We thus repeated the cross power spectral analysis excluding the stations TAR, NUR and HAN, which lie in this latitude range, i.e. the cross power spectra for the H and D components were recomputed from the MM100 stations THY, NCK, BEL, SOD, and KIL. The cross power spectra computed in this way (not shown) were very similar to those in Fig. 1 and still clearly showed power at lower frequencies, especially around 20 mHz in the D component, thus confirming that it is not related to a FLR.

We next consider more detailed spectra for two shorter time intervals, one before the decrease and one following the decrease in B_{IMF}, at one of the low latitude stations, HER. The MESA dynamic spectra for the 20 min interval 08:50–09:10 UTC for the H and D components observed at Hermanus are plotted in Fig. 2a. Each individual spectrum was computed using a prediction error filter of order 30 with a 90 s data window, which was progressively shifted by 10 s (see Ndiitwani and Sutcliffe, 2009, for computational details). The MESA dynamic spectra have an effective time resolution (90 s) that is much higher than that of the FFT dynamic spectra (10 min). This allows the finer structure of the various signals to be seen and shows that they actually have an intermittent nature and variable frequency; this type of fine structure was previously reported for UWs and FLRs by Verõ et al. (1998) using a different method of analysis. In Fig. 2b the FFT amplitude spectra for the 5 min subinterval 08:55–09:00 UTC are plotted. These and other similar spectra were smoothed using five spectral estimates, i.e. computed with 10 degrees of freedom. The reason for selecting such a short time interval is that, due to the variable nature of the signals, FFT amplitude spectra computed over longer intervals resulted in smoothed spectra, which did not necessarily clearly show the presence of signals from the three

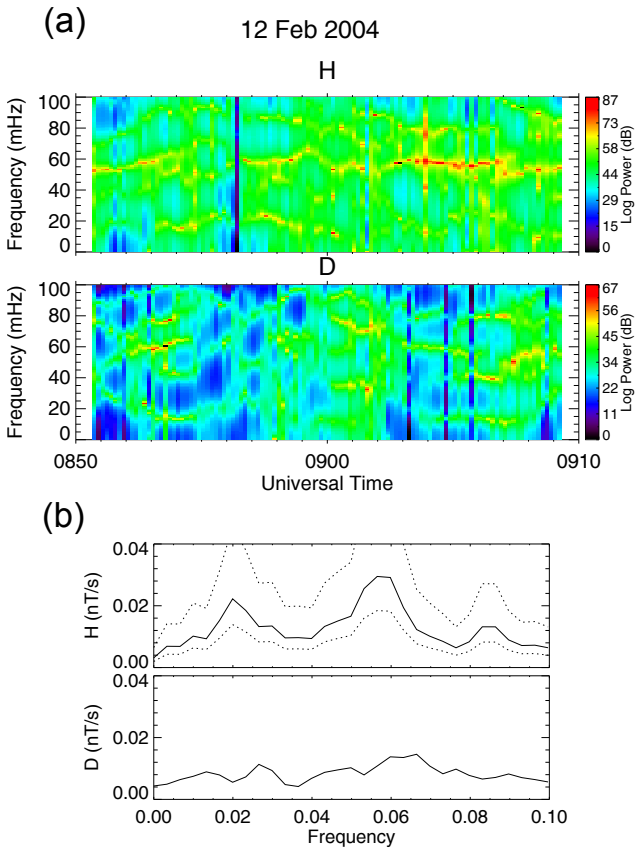

Fig. 2. (a) MESA dynamic spectra for the 20 min interval 08:50–09:10 UTC for the H and D components observed at Hermanus prior to the decrease in B_{IMF} and **(b)** the FFT amplitude spectra for the 5 min subinterval 08:55–09:00 UTC.

sources. Furthermore, the particular 5 min interval was selected for a time when signals from all three of the sources appeared to be present in the MESA spectra. Thus, for example, the signal close to 20 mHz is not clear in the MESA spectra during the interval 09:00–09:05 UTC and was consequently not clearly evident in the FFT amplitude spectra for this interval. The dotted curves in the upper H component panel show the 80 % confidence limits, i.e. with 80 % confidence the true spectral estimates lie in the region between dotted curves. Since the maxima of the lower and minima of the upper dotted curves lie above and below the valleys and peaks in the amplitude spectrum, the three spectral peaks can be regarded as statistically significant. The FLR identified in the top panel of Fig. 1 is observed close to 58 mHz in both H component spectra. Note, however, that in the MESA spectrum the signal is intermittent with slightly variable frequency, which is typical of the packet structure of Pc3–4 FLRs (Verõ and Miletits, 1994). During this interval the computed UW frequency $6 \cdot B_{IMF} \sim 75$ mHz. The UW signal is seen as intermittent power between 75 and 85 mHz in the MESA spectra and as a peak at 85 mHz in the FFT H component spectrum. Oscillations at lower frequencies, although

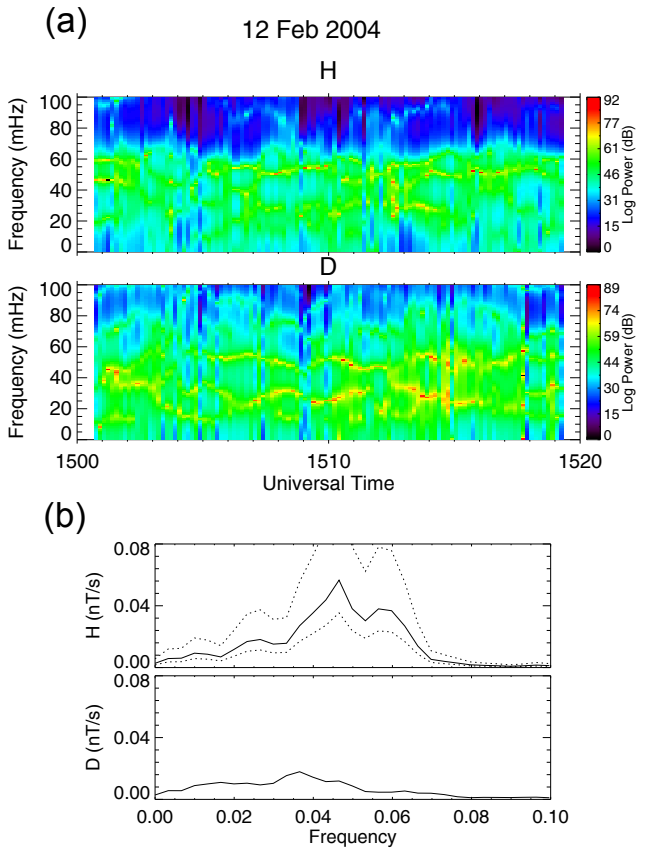

Fig. 3. (a) MESA dynamic spectra for the 20 min interval 15:00–15:20 UTC for the H and D components observed at Hermanus following to the decrease in B_{IMF} and **(b)** the FFT amplitude spectra for the 5 min subinterval 15:00–15:05 UTC.

variable and intermittent, are also clear in the MESA spectra and tend to repeat close to certain frequencies, particularly around 20 mHz in the H component. An intermittent signal is observed close to 40 mHz in the D component spectrum at 08:53–08:55, 09:00–09:02, and 09:05–09:07 UTC. The 20 mHz peak is also clear in the FFT H component spectrum. Clearly, these signals are not directly related to the higher frequency FLR or UW signals; consequently, we suggest that they provide possible evidence of FMRs as observed in Fig. 1.

MESA and FFT spectra similar to those in Fig. 2 are plotted in Fig. 3 for an interval following the decrease in B_{IMF}. Figure 3a shows the MESA dynamic spectra for the 20 min interval 15:00–15:20 UTC for the H and D components at HER. Figure 3b shows the FFT amplitude spectra for the 5 min subinterval 15:00–15:05 UTC, when signals from the three sources appear to be present. The previously identified FLR is again evident in both H component spectra; it is seen as an intermittent and variable signal between 55 and 60 mHz in the MESA spectrum and as a broad peak between 57 and 60 mHz in the FFT amplitude spectrum. During this interval the computed UW frequency had decreased to $6 \cdot B_{\mathrm{IMF}} \sim 43$ mHz, thus power at higher frequencies is significantly less than in Fig. 2. The UW signal appears as intermittent power between 45 and 52 mHz in the MESA spectra and as a peak at 46 mHz in the H component FFT spectrum. Although the separation between the two peaks in the latter spectrum is not statistically significant, we believe them to be real based on the physics of the situation. Since the FLR and UW frequencies were very close together at this time, some further comments on the MESA H component spectrum are in order. During the first few minutes the two frequencies are clearly resolved. During the interval 15:05–15:10 UTC they appear to have merged into a single peak in the dynamic spectrum. During the interval 15:10–15:20 UTC there appears to be some alternation between the two signals, similar to that reported for FLRs and UWs by Verõ et al. (1998). Oscillations at lower frequencies are again observed. In the MESA spectra they vary between 10 and 30 mHz while power in this frequency band is also evident in the FFT H component spectrum. We suggest that this might again be indicative of an FMR.

Figure 4a shows the H component FFT spectra, smoothed using 10 spectral estimates, for all eight MM100 stations for the interval 15:00–15:20 UTC, i.e. the same interval as the Hermanus MESA dynamic spectra in Fig. 3a. The motivation for Fig. 4a is different from that of Figs. 2 and 3. The objective is to show the ubiquitous presence of clear peaks at the previously inferred FMR frequencies in the spectra at all the MM100 stations. The figure furthermore illustrates the latitude independence of the peaks and that they lie far from the expected UW frequency. The clearest peak is observed at ~ 27 mHz. Other peaks are evident at around 10 mHz, and 20–23 mHz. The UW related peak is less clear at 45–50 mHz in each individual spectrum. The relative spectral peak heights are influenced by local field line resonances (e.g. the highest peak at BEL is at ~ 27 mHz, at TAR at ~ 20 mHz, at NUR at ~ 10 mHz and at HAN at ~ 8 mHz), and possibly also by the spatial structure of the resonance as discussed later in the discussion section. FFT D component spectra for the same event (not shown) were computed in the same way. These show the largest and clearest peak at ~ 27 mHz at all stations. The other peaks observed in the H component are not as evident in the D component spectra. We believe that these observations suggest that the FMR should play a role in redistributing the ULF wave energy in the magnetosphere. Figure 4b shows the H component spectrum for NUR, computed without any filtering or time differencing, plotted on a log-log scale. The low frequency peaks identified in Fig. 4a are clearly evident in Fig. 4b, thus confirming that they are real and not an artefact of the filtering process.

The results presented above indicate that the Pc3–4 pulsation spectra contain an UW contribution with frequency related to B_{IMF}, an FLR contribution with latitude dependent frequency, plus other structure. In the past, a number of researchers have shown that the FLR peaks in Pc3 spectra

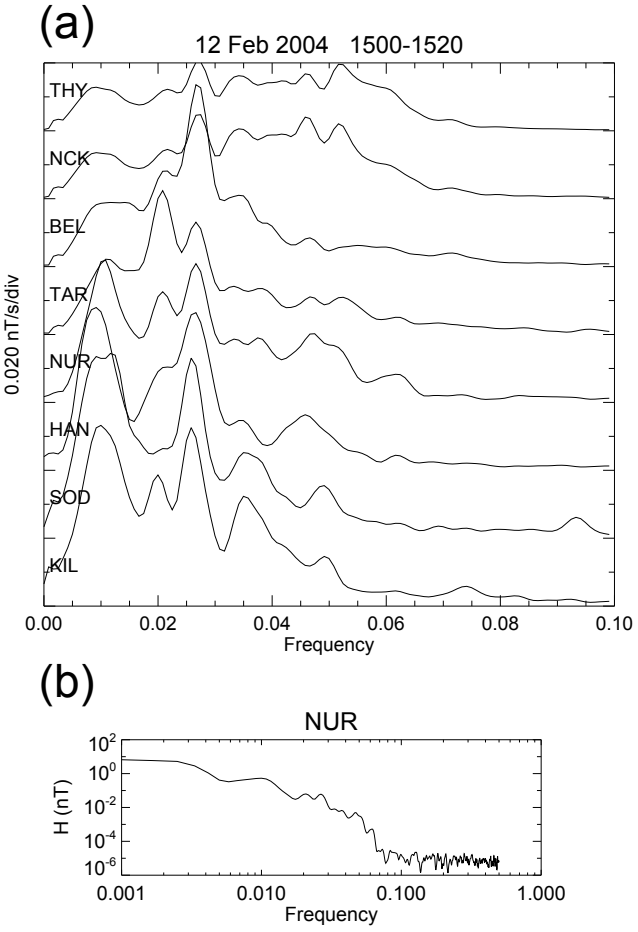

Fig. 4. (a) FFT amplitude spectra for the H component at the MM100 stations for the 20 min interval 15:00–15:20 UTC and **(b)** H component spectrum for NUR, computed without any filtering or time differencing.

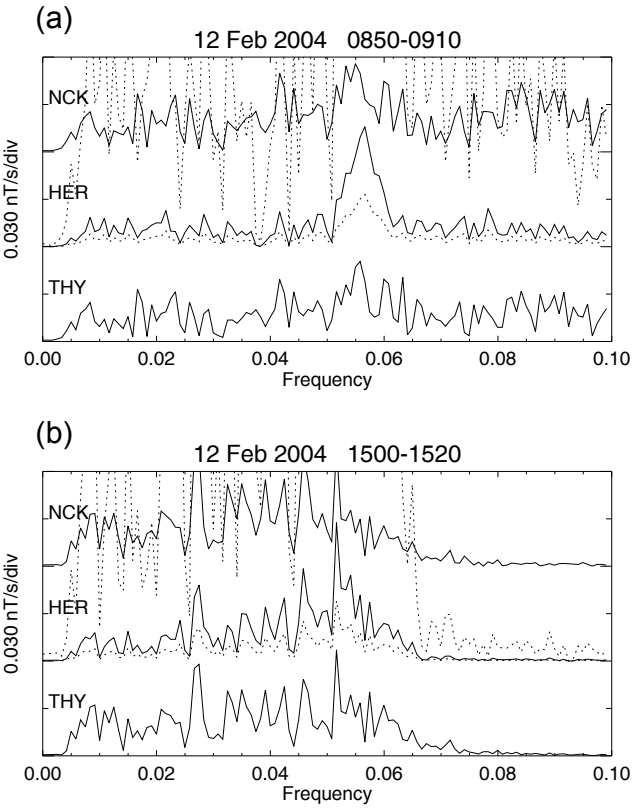

Fig. 5. High resolution FFT H component amplitude spectra for the 20 min intervals **(a)** 08:50–09:10 UTC and **(b)** 15:00–15:20 UTC prior to and following the decrease in B_{IMF}, respectively, on 12 February 2004 at THY, HER, and NCK. The dotted curves show the 80 % confidence limits for the HER spectra.

contain a fine structure and suggested that these FLRs are coupled to compressional cavity or waveguide modes (Samson et al., 1995; Menk et al., 2000). Samson et al. (1995) pointed out that this fine structure will be easily missed if the spectra are computed with an inappropriate choice of parameters, such as a spectral smoothing window that is too wide (e.g. greater than 1or 2 mHz) or where the power spectra are plotted on a logarithmic scale. However, as pointed out in Sect. 2.3 above, spectra computed in this way are highly unstable and the individual peaks unlikely to be statistically significant. Menk et al. (2000) state that their spectra, computed from time series of length 20 min and $\Delta t = 2$ s, had a resolution of ~ 0.8 mHz. This implies that the spectra were computed without any averaging and thus with $n = 2$ degrees of freedom. In order to test whether we could observe similar fine structure in our data, we recomputed some of the FFT spectra with greater spectral resolution in a manner similar to Menk et al. (2000). This was achieved by computing FFT spectra for the 20 min intervals used in Figs. 2a and 3a for three of the low latitude stations with no averaging of spectral estimates. The H component spectra for THY, HER, and NCK for the two 20 min intervals are plotted as solid curves in Figs. 5a and b, respectively. The dashed curves indicate the 80 % confidence limits for the HER spectra, i.e. centre solid curve. As was the case with the spectra presented by Menk et al. (2000), the most striking aspect of the spectra is the appearance of common peaks across stations and the narrow and consistent spacing between many of these peaks, particularly in Fig. 5b. However, it is also clear that very few of these peaks are statistically significant. The only individual peaks for HER in Fig. 5a that might be regarded as statistically significant are those at 42 and 58 mHz, the former close to the FMR frequency in the H componnent cross power panel in Fig. 1 and the latter equal to the FLR frequency in Figs. 2a and b. In Fig. 5b none of the individual peaks are statistically significant; however, the frequencies of the larger peaks at 27 and 46 mHz agree with those of the FMR and FLR in the averaged FFT spectrum in Fig. 3b.

In the experiments carried out by Ndiitwani and Sutcliffe (2009) on synthetic signals using MESA, they found that it is necessary to increase the PEF order as more noise was added

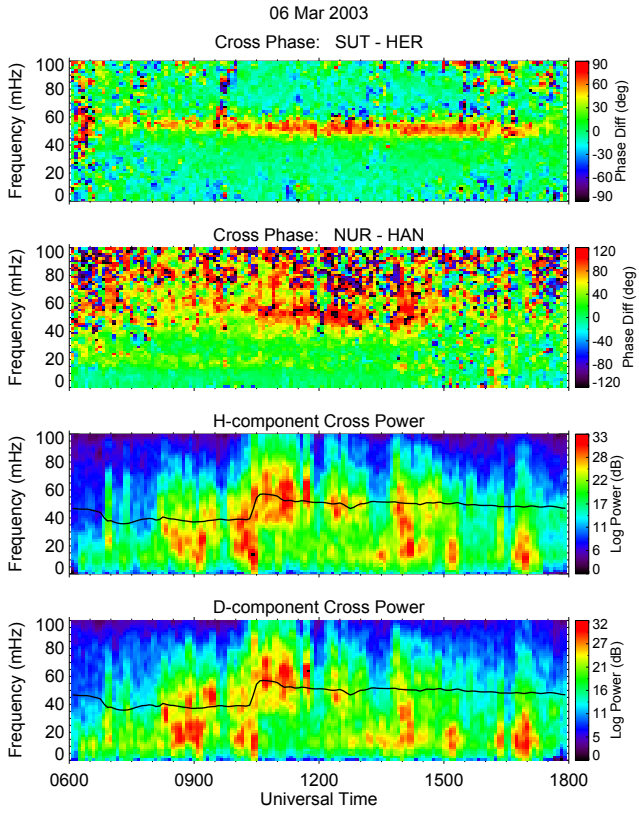

Fig. 6. Dynamic FFT cross phase and power spectra for the Pc3–4 pulsation activity observed during the interval 06:00–18:00 UTC on 6 March 2003. The cross power spectra were computed from all eight of the MM100 stations listed in Table 1.

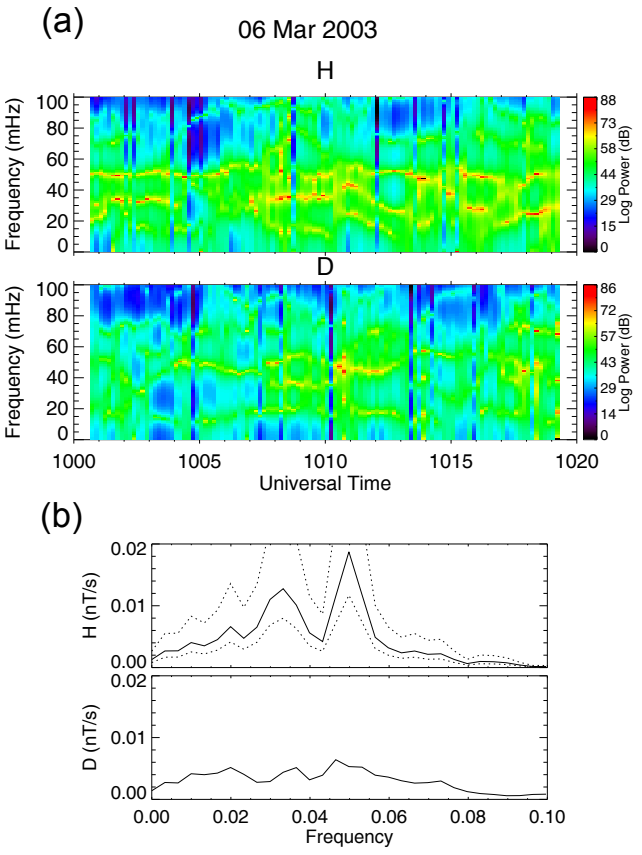

Fig. 7. (a) MESA dynamic spectra for the 20 min interval 10:00–10:20 UTC for the H and D components observed at Hermanus shortly before increase in B_{IMF} and **(b)** the FFT amplitude spectra for the 5 min subinterval 10:00–10:05 UTC.

or if one of the signal amplitudes was very much smaller than the others. Consequently, in order to determine whether we could identify any fine structure in Pc3–4 pulsations using MESA, we repeated the analyses shown in Figs. 2a and 3a with increased PEF order. We increased the order in steps of 5 from 30 to 85. (Note that an order of 90 or greater, i.e. equal to the number of data points in the time series, is not possible since this leads to singularities when solving the PEF matrix equations.) We found that the main structures in the dynamic spectra remained essentially the same and there was no evidence of any fine structure. We also inspected individual MESA spectra and found that for the larger orders, the most intense peak in the spectrum, e.g. the 58 mHz peak seen in Fig. 2a, split into two. In addition, one or two additional peaks developed at the low or high frequency ends of the spectrum; however, there was no evidence of any fine structure.

3.2 Event of 6 March 2003

The second event that we consider occurred on 6 March 2003, when the IMF total $\boldsymbol{B}$ field increased by about 3 nT within 5 min. Dynamic cross phase and power spectra for the ground-based Pc3–4 pulsation activity observed during the interval 06:00–18:00 UTC are presented in Fig. 6 in the same format as Fig. 1. The top panel shows the occurrence of a field line resonance for the SUT–HER station pair, which decreased from 55 to 50 mHz through the day. The second panel indicates the occurrence of a field line resonance with harmonic structure for the NUR–HAN station pair, in which the fundamental frequency decreased from about 20 to 15 mHz through the day.

The lower two panels show the cross power for the H and D components, respectively, computed from all eight of the MM100 stations listed in Table 1. Power around the estimated UW frequencies, i.e. which tends to straddle the superimposed black curves in the H and D component panels, is evident and clearly increased in frequency when the estimated UW frequency increased. The cross power spectra also clearly show oscillations at other frequencies, which are not directly related to UW activity or FLR structure. A broad band of activity around 20 mHz is very clear throughout the day. We again repeated the cross power spectral analysis excluding the stations in the $L = 3$ range, whose fundamental FLR frequency lies around 20 mHz. The cross power spectra

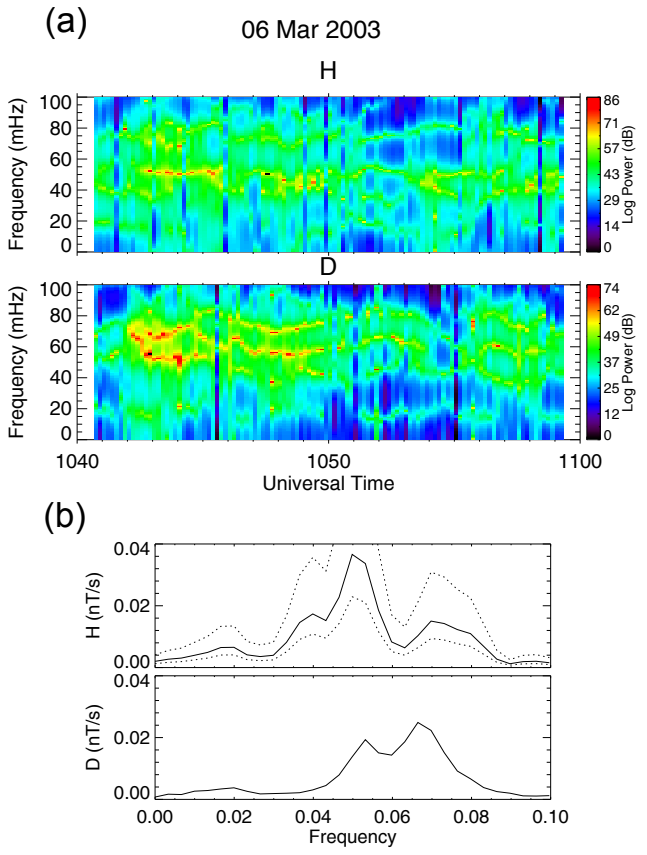

Fig. 8. (a) MESA dynamic spectra for the 20 min interval 10:40–11:00 UTC for the H and D components observed at Hermanus immediately following the increase in B_{IMF} and **(b)** the FFT amplitude spectra for the 5 min subinterval 10:40–10:45 UTC.

for the H and D components computed from the MM100 stations THY, NCK, BEL, SOD, and KIL (not shown) were very similar to those in Fig. 6, confirming that these frequencies are common to all stations and which we ascribe to an FMR.

We next consider more detailed spectra for two shorter time intervals, one shortly before and one shortly after the increase in B_{IMF}, at one of the low latitude stations. The MESA dynamic spectra for the 20 min interval 10:00–10:20 UTC for the H and D components observed at HER are presented in Fig. 7a. The FFT amplitude spectra for the 5 min subinterval 10:00–10:05 UTC are presented in Fig. 7b. The previously identified FLR at 50 mHz is clear in both H component spectra. During this interval the computed UW frequency $6 \cdot B_{\mathrm{IMF}} \sim 39$ mHz. The UW signal is clearly evident at 33 mHz in both H component spectra; it manifests itself as intermittent power in the MESA spectrum and as a peak in the FFT spectrum. It also appears in the MESA D component spectrum for a short time from 10:08–10:11 UTC, when it is most intense in the MESA H component spectrum. Oscillations at other frequencies also occur in the spectra. A signal around 20 mHz, which is variable and intermittent, is evident in the MESA D component and manifests itself as small peaks, although not statistically significant, in both the H and D component FFT spectra. An oscillation around 45 mHz is also observed as a variable and intermittent signal in the MESA D component spectrum and as a peak in the FFT D component spectrum. We again suggest that these additional signals provide possible evidence of FMRs.

Spectra similar to those in Fig. 7 are presented in Fig. 8 for an interval immediately following the increase in B_{IMF}. The MESA dynamic spectra for the 20 min interval 10:40–11:00 UTC for the H and D components at HER are shown in Fig. 8a. Figure 8b shows the FFT amplitude spectra for the 5 min subinterval 10:40–10:45 UTC. The 50 mHz FLR is again evident in both H component spectra. During this interval the estimated UW frequency had increased to $6 \cdot B_{\mathrm{IMF}} \sim 57$ mHz. The UW signal manifests itself as variable power between 70 and 80 mHz in the MESA H and D component spectra and as a broad peak in the FFT H and D component spectrum. Although these frequencies appear to be substantially higher than the estimated UW frequency, they fall within the range of UW frequencies expected for the observed B_{IMF} as determined by Yumoto et al. (1984). Oscillations at lower frequencies are again observed. In both of the MESA components and in the FFT H component spectra, weak signals occur at 40 and 20 mHz, which we ascribe to FMRs. The dotted curves in the upper H component panels in Figs. 7b and 8b show the 80 % confidence limits. It is seen that the spectral peaks associated with the FLR and UW activity are statistically significant. However, the peaks that we ascribe to FMR activity are not statistically significant in this example; this may be as a result of the variable frequency and intermittent nature of the signals.

For this event we again present a stacked plot of spectra for the MM100 stations computed for the 30 min interval 08:50–09:20 UTC when significant power was observed around 20 mHz in the dynamic cross power spectra in Fig. 6. The FFT amplitude spectra for the D component plotted in Fig. 9a show clear latitude independent peaks at ~ 15, ~ 23, ~ 40, and ~ 48 mHz at all stations, although the latter two are less evident below $L = 2$. Each of the peaks had its maximum at the highest latitude station. The peak at ~ 40 mHz corresponds to the UW related activity. At all stations the strongest peaks are those at ~ 15 mHz and ~ 23 mHz, which are clearly not related to UWs or FLRs. The H component spectra (not shown) tend to be dominated by local FLR signals. Figure 9b shows the D component spectrum for THY, computed without any filtering or time differencing, plotted on a log-log scale. Figure 9b serves as confirmation that the low frequency peaks in Fig. 9a are real and not an artefact of the filtering process.

We again did a test to determine whether we observe fine structure in FLR peaks as reported by Samson et al. (1995) and Menk et al. (2000). We computed the FFT spectra for the 20 min intervals used in Figs. 7a and 8a for the three low latitude stations THY, HER, and NCK with greater spectral

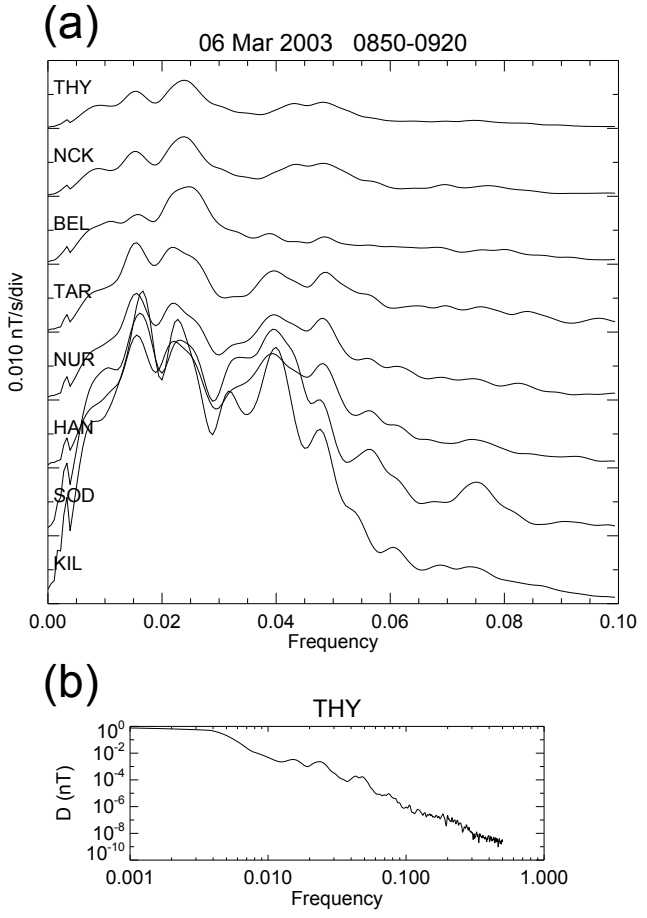

Fig. 9. (a) FFT amplitude spectra for the D component at the MM100 stations for the 30 min interval 08:50–09:20 UTC and **(b)** D component spectrum for THY, computed without any filtering or time differencing.

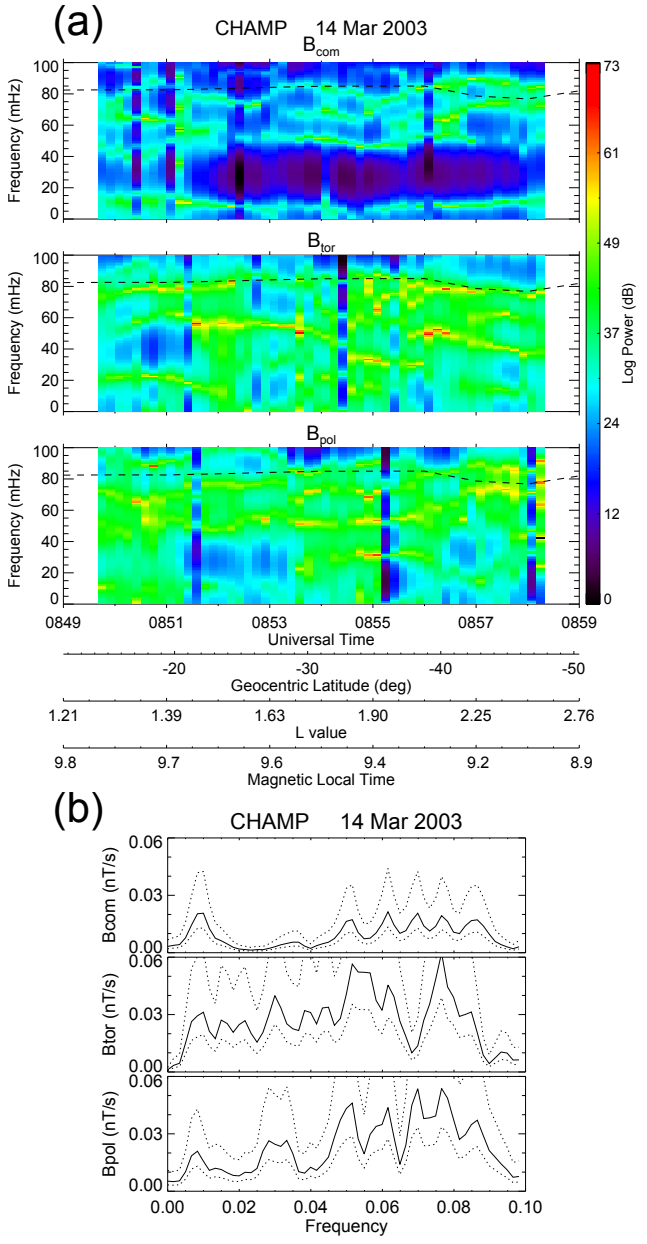

Fig. 10. (a) MESA dynamic spectra and **(b)** FFT averaged spectra for the CHAMP compressional ($B_{\rm com}$), toroidal ($B_{\rm tor}$), and poloidal ($B_{\rm pol}$) components observed on 14 March 2003 during the interval 08:49–08:59 UTC when the estimated UW frequency $6 \cdot B_{\rm IMF} \sim 83$ mHz.

resolution, i.e. with no averaging of spectral estimates, in a manner similar to that in Fig. 5. The H component spectra (not shown) again exhibited common peaks across stations with narrow spacing between many of the peaks; however, the fine structure within the broader FLR peaks was not statistically significant for any of the peaks.

4 CHAMP observations

We next consider the spectral structure of three events observed in magnetic field data from the fluxgate magnetometer onboard CHAMP and simultaneously at ground stations closely traversed by CHAMP.

4.1 Event of 14 March 2003

The first event utilising satellite data occurred on 14 March 2003, when the estimated UW frequency $6 \cdot B_{\rm IMF} \sim 83$ mHz and the CHAMP orbit crossed the Hermanus L shell within 2° of longitude. MESA dynamic spectra and FFT averaged spectra are shown in Figs. 10a and b, respectively, for the CHAMP compressional ($B_{\rm com}$), toroidal ($B_{\rm tor}$), and poloidal ($B_{\rm pol}$) components observed during the interval 08:49–08:59 UTC. The MESA dynamic spectra were computed in a manner similar to that used for the ground-based data in Sect. 3.1 (see Ndiitwani and Sutcliffe, 2009, for computational details). The dynamic spectra enable both shear Alfvén and fast mode waves to be

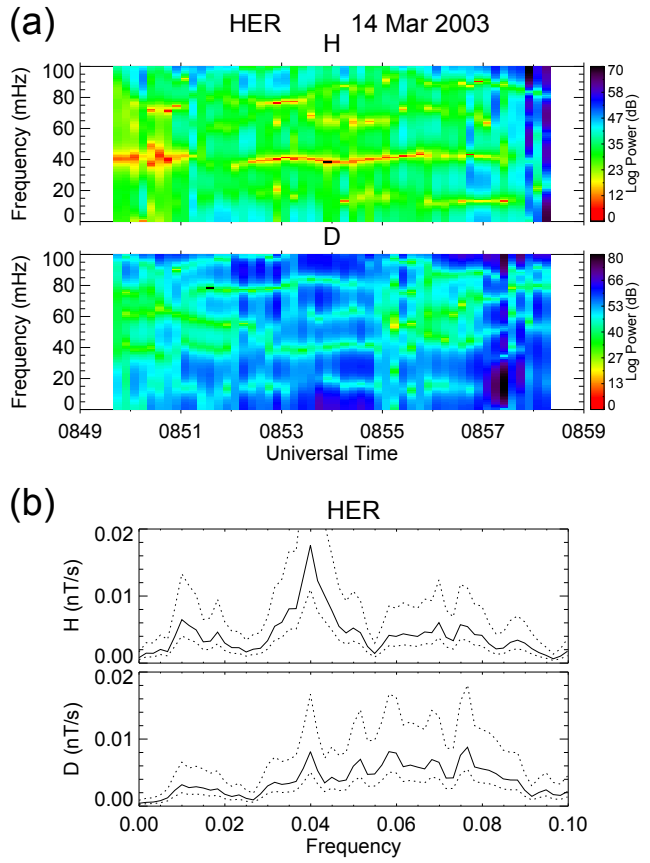

Fig. 11. (a) MESA dynamic spectra and **(b)** FFT averaged spectra for the HER *H* and *D* components observed on the ground at the same time as the CHAMP data in Fig. 10.

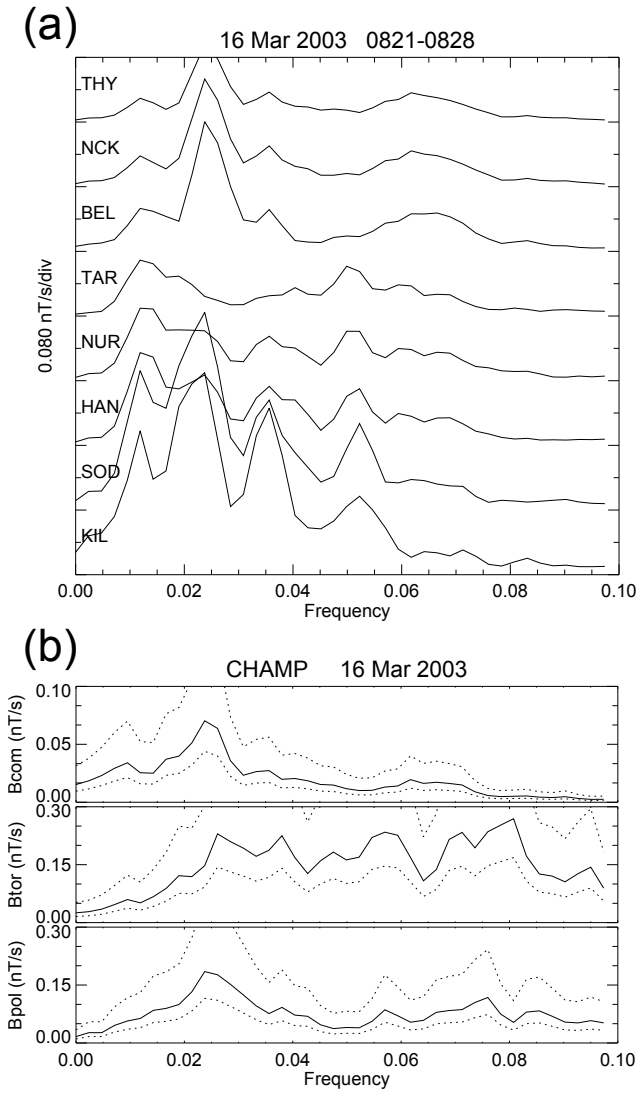

Fig. 12. (a) FFT amplitude spectra for the *D* component at the MM100 stations for the 7 min interval 08:21–08:28 UTC on 16 March 2003 and **(b)** FFT averaged spectra for the CHAMP compressional (B_{com}), toroidal (B_{tor}), and poloidal (B_{pol}) components for the same interval.

observed; however, as explained by Vellante et al. (2004), FLRs observed on the satellite will undergo a Doppler shift relative to the resonance frequency observed on the ground as a result of the rapid motion of the satellite across the resonance region. The FFT averaged spectra in Fig. 10b were computed as previously described in Sect. 3.1 with smoothing over five spectral estimates. MESA dynamic spectra and FFT averaged spectra for the HER ground station for the same time interval are shown in Figs. 11a and b, respectively.

There is evidence of an FLR in the CHAMP B_{tor} component dynamic spectrum in Fig. 10a, e.g. the 33 mHz signal at 08:55 UTC is a Doppler shifted FLR associated with the intense 40 mHz FLR observed in the HER ground data in Fig. 11. The FLR frequency increases toward lower latitudes. The latitude dependent frequency (55–40 mHz) observed between 08:56–08:58 UTC is likely the second harmonic of an FLR at higher latitudes. The dynamic spectra for B_{com} and B_{pol} show that a number of signals, which vary in frequency and intensity, tend to persist in the fast mode components as CHAMP rapidly moves across *L* shells. Besides the peak at $\sim$ 86 mHz, close to the computed UW frequency, the FFT averaged spectra for B_{com} and B_{pol} have clear peaks at $\sim$ 50, $\sim$ 62, $\sim$ 70, $\sim$ 77 mHz, some of which may arise due to the variability of the signal frequencies seen in the dynamic spectra. In other events (not shown) we also noted a tendency for there to be a greater number of peaks in the FFT averaged spectra than in the MESA dynamic spectra, where the signals appeared to vary in frequency and intensity. Some of these peaks are also observed in the B_{tor} component. However, we again suggest that these signals may be due to FMRs. Peaks with frequencies close to those in the CHAMP averaged spectra are also observed on the ground, particularly in the HER *D* component. We also note that the fast mode signals in the high frequency part of the spectra,

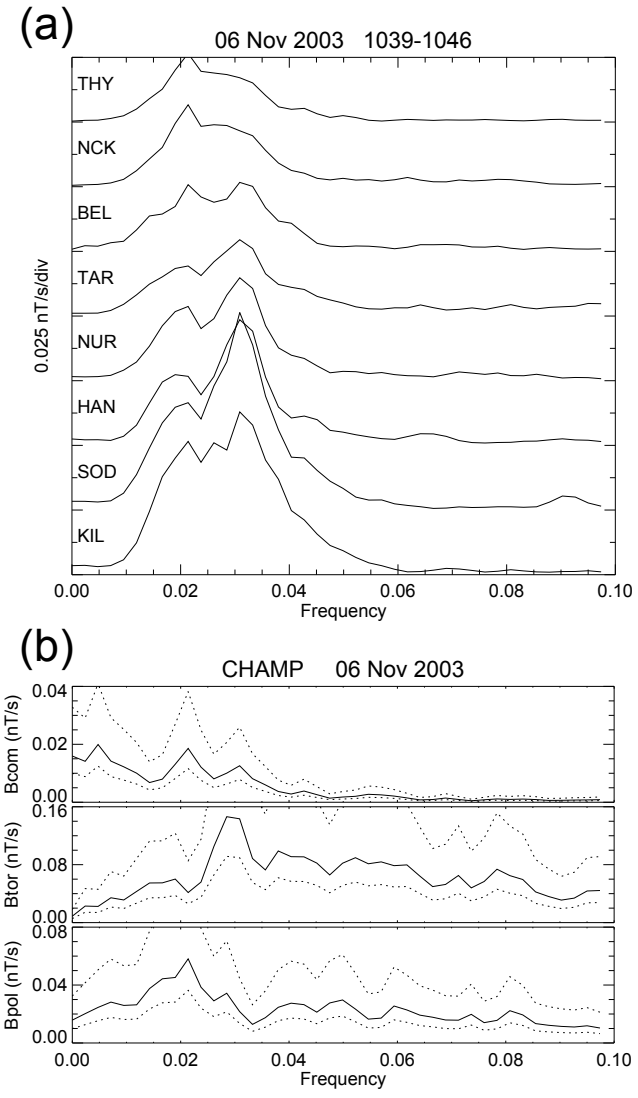

Fig. 13. (a) FFT amplitude spectra for the D component at the MM100 stations for the 7 min interval 10:39–10:46 UTC on 6 November 2003 and **(b)** FFT averaged spectra for the CHAMP compressional (B_{com}), toroidal (B_{tor}), and poloidal (B_{pol}) components for the same interval.

i.e. those closer to the UW frequency (see black dashed lines at $6 \cdot B_{\mathrm{IMF}} \sim 83$ mHz), tend to be more prominent.

4.2 Event of 16 March 2003

The second of the events utilising CHAMP data with simultaneous ground magnetometer data occurred on 16 March 2003. FFT amplitude spectra, with averaging over five spectral estimates, were computed for the 7 min time interval 08:21–08:28 UTC when CHAMP was crossing over the MM100 chain within 10° of longitude.

The D component spectra for all MM100 stations are presented in Fig. 12a. The peaks at ~ 36 mHz observed at all stations except TAR, when the estimated UW frequency $6 \cdot B_{\mathrm{IMF}} \sim 40$ mHz, are ascribed to UWs. We believe that the clear, sharp peaks at ~ 24 mHz, which are observed at all stations except TAR, to be due to an FMR. It is not clear whether the small peaks close to 12 mHz are real or whether they arise due to the filter cut-off; spectra of unfiltered data plotted on log-log scales did not show clear peaks at all stations. In addition, a broad peak is observed close to 62 mHz at the three lower latitude stations and a clear peak around 51 mHz is observed at the five higher latitude stations.

The CHAMP compressional (B_{com}), toroidal (B_{tor}), and poloidal (B_{pol}) component spectra are presented in Fig. 12b; note the more sensitive amplitude scale for B_{com}. The low frequency peaks at ~ 10 mHz in B_{com} and B_{tor} are probably due to the satellite rapidly traversing lithospheric anomalies, which results in an apparent signal in the Pc4 and Pi2 frequency bands (Sutcliffe and Lühr, 2003). The CHAMP compressional and poloidal component FFT spectra both show clear peaks, which are statistically significant, at ~ 24 mHz, that is, at the same frequency as the largest peaks in the ground station spectra, which we ascribe to an FMR. The small peaks between 36–38 mHz are probably of upstream origin. The compressional component also shows a broad peak around 62 mHz, which is not statistically significant, as was observed at the lower latitude ground stations.

4.3 Event of 6 November 2003

The third event that we consider utilising CHAMP data occurred on 6 November 2003, 10:39–10:46 UTC, when the estimated UW frequency $6 \cdot B_{\mathrm{IMF}} \sim 27$ mHz. Spectra for the MM100 stations and CHAMP for this event are presented in Fig. 13 in the same format as in Fig. 12; note the different amplitude scales used in the CHAMP component spectra.

The peaks around 30 mHz in the MM100 ground station D component spectra and in the spectra of all components on CHAMP lie close to the computed UW frequency and can thus be ascribed to UWs. Clear peaks are observed at ~ 22 mHz in the D component spectra of all MM100 ground stations and in the spectra of the compressional and poloidal components on CHAMP. The compressional component peak, although weaker than the poloidal component peak, is statistically significant. We believe the 22 mHz signal to provide convincing evidence of an FMR signature.

5 Conclusions and discussion

It is commonly accepted that field line resonances (FLRs) excited by fast mode waves in the plasmasphere are the prime source of Pc3–4 pulsations observed at low and middle latitudes during local daytime (Menk et al., 1994). It is also widely accepted that the source of the fast mode waves responsible for driving the FLRs are upstream waves generated by an ion cyclotron instability driven by ion beams reflected from the bow shock region (Le and Russell, 1994).

Contrarily, a number of investigators have suggested that FMRs due to cavity or waveguide modes in the plasmasphere are the drivers of the FLRs (Allan et al., 1985; Samson et al., 1995; Waters et al., 2000; Menk et al., 2000). However, clear observational evidence for FMRs is rather limited (Waters et al., 2002).

In this study we investigated the spectral structure of Pc3–4 pulsations observed at low and midlatitudes. In order to do this, fluxgate magnetometer data recorded at the MM100 stations in Europe (Heilig et al., 2007) and induction magnetometer data recorded at two low latitude stations in South Africa were used. In addition, fluxgate magnetometer data from the CHAMP low Earth orbit (LEO) satellite (Reigber et al., 2002) were used. The results of our analysis suggest that at least three mechanisms contribute to the spectral content of Pc3–4 pulsations typically observed at low and midlatitudes. We confirmed that a typical Pc3–4 pulsation contains a field line resonance (FLR) contribution with latitude dependent frequency. For ground-based data, the cross-phase method (Waters et al., 1991) was used to isolate the presence of FLRs. In the CHAMP data, the FLR could be identified in the toroidal component as an oscillation that is Doppler shifted relative to the FLR observed when crossing the ground station. The Pc3–4 pulsations also typically contain an upstream wave (UW) contribution with frequency proportional to the IMF magnitude B_{IMF}. We used two approaches to identify the presence of UWs in the ground station data; the first was to select data for days where the IMF total $\boldsymbol{B}$ field varied significantly while the second was based on determining the cross power from a meridian chain of stations as used by Heilig et al. (2007). In the CHAMP data, the UW contribution could be identified as peaks in the spectra close to the computed frequency $6 \cdot B_{\mathrm{IMF}}$ mHz. Besides the FLR and UW contributions, the Pc3–4 pulsations consistently contain signals at other frequencies. In particular, we presented examples which show the ubiquitous presence of clear peaks in the spectra at all the MM100 stations and at CHAMP. We furthermore showed that these peaks are independent of latitude and that they differ from the expected UW frequency. We suggest that the most likely explanation for these additional frequency contributions is that they are fast mode resonances (FMRs) related to cavity, waveguide, or virtual modes. Although the above contributions to Pc3–4 spectral structure have been reported previously, we believe that this is the first time where evidence of their simultaneous presence in both ground-based and satellite data has been presented.

Verõ et al. (1998) made a detailed study of UWs and FLRs in Pc3 pulsation events at a ground station array between $L = 1.5$ and 3 in central Europe. They separated the UW and FLR contributions using the frequency structure of the pulsations across the stations, i.e. the UW frequency was stationary over short time intervals while the FLR frequency decreased with increasing L value. Verõ et al. (1998) found that UW events were imbedded in intervals of strong pulsation activity, even if the activity was mostly of FLR origin. The two types, FLR and UW activity, may alternate quite quickly, i.e. within a few minutes, but they may also appear simultaneously. UW events are strong, but are of short duration with variable period, while FLR activity is nearly always present to a certain degree. There are some similarities between the results of Verõ et al. (1998) and our results. For example, our MESA dynamic spectra for both ground station and CHAMP data show multiple frequency structures that vary with time. These variations resemble the intermittent nature and variations in period observed by Verõ et al. (1998) in their ground array pulsations.

We discuss our observations of suggested FMRs in the light of theoretical models and observations previously reported in the literature. A number of models have been developed showing that the fast compressional mode can drive resonant cavities, which form between a reflecting outer boundary, such as the magnetopause or plasmapause, and the surface of the turning points deeper within the magnetosphere where the radial wave-number becomes zero. Energy from the compressional wave-guide modes can also tunnel to field lines earthward of the turning point to drive discrete shear Alfvén mode resonances where their eigenfrequencies match those of the fast modes (Samson et al., 1995). Some of the earlier models were those of Kivelson and Southwood (1985), who used a simple box model of the magnetosphere, Allan et al. (1985, 1986a, b), who used an infinitely long half-cylinder magnetosphere model, while Samson et al. (1995) used a WKB (Wentzel–Kramers–Brillouin) analysis of a wave-guide mode to show that damped, fast eigenmode solutions with quantized frequency are produced. The model of Allan et al. (1986b) showed that the compressional component periods are virtually constant over the whole range of radial distance, which they interpreted as standing-wave harmonics in the magnetospheric cavity. The periods of the first four cavity resonance harmonics in the Allan et al. (1986b) model were 90, 46, 31, and 24 s, i.e. 11.1, 21.7, 32.3, and 41.7 mHz, respectively. We suggest that the signals in our spectra, which have latitude independent frequencies similar to those above at the MM100 stations and which tend to persist in the fast mode components as CHAMP rapidly moves across L shells, could also be interpreted as similar standing-wave harmonics. The models of Allan et al. (1985, 1986b) also showed that the transverse mode consists of two components. The one has a period which varies with radial distance and is virtually the same as the uncoupled toroidal mode period; this is what we observe as a FLR. The other has virtually constant period with radial distance, which they call the monochromatic transverse component, and whose period is identical to that of the fundamental fast eigenmode. The signals in the B_{tor} component of our dynamic spectra with quasi-constant frequency as CHAMP rapidly moves across L shells may be evidence of this monochromatic transverse component. Allan et al. (1986a) extended their model to include a plasmapause in the magnetospheric cavity. They found that the plasmapause

plays a pivotal role in determining which compressional cavity resonances are dominant. The critical factor is whether a node of a particular cavity resonance lies on or near the plasmapause, in which case the resonance is enhanced; otherwise, it is attenuated. In particular, they found that the fundamental cavity resonance, which does not have a node within the magnetospheric cavity, is always suppressed relative to its dominance in the case with no plasmapause. Consequently, the introduction of a plasmapause results in the second harmonic, with frequency close to 20 mHz having the largest amplitude. In most of our examples, the fast mode signal with frequency close to 20 mHz was the clearest.

Theoretical studies in the past have shown that the plasmapause cannot be treated as a perfect reflector of compressional waves. The properties of the resonances are strongly controlled by both the radial Alfvén speed profile and the ionospheric conditions. The plasmaspheric virtual mode resonance (VMR) was found to be a better description of the results of theoretical models using a realistic plasmapause. According to Lee and Takahashi (2006) the fundamental mode frequency of a VMR could range from a few mHz to several 10's of mHz. The spacing between the adjacent harmonics is also very variable ($\sim$ 6–15 mHz in their examples), and strongly depends on the properties of the medium.

Lee and Takahashi (2006) also presented the spatial structure of the VMR (see their Plates 3 and 4). Based on their results the fundamental mode of a VMR is not expected to be observed in the compressional (parallel) component near the plasmapause. Most of the wave energy in the compressional component is concentrated to lower latitudes. Contrarily, the VMR has a node in the radial (poloidal) component at the equator, and peaks near the plasmapause. The VMR poloidal component extends beyond the plasmapause. The nodal structure of the VMR may explain why some of the resonant peaks could not be observed in the compressional component in CHAMP's dynamic spectra, while they appeared clearly in the poloidal component (e.g. Fig. 10a). The same spatial structure cannot be observed in the FFT spectra of the CHAMP components, since these are averaged over a wide range of latitudes. However, the ratio of these averaged amplitudes seems to be fairly stable (B_{pol} being typically 2–3 times larger than B_{com}), as expected for a resonant structure.

The plasmapause positions for the events considered were calculated based on the Carpenter and Anderson (1992) model, i.e. $L_{\mathrm{pp}} = 5.6\text{–}0.46 \cdot K_{\mathrm{pmax}}$, where K_{pmax} is the maximum of K_{p} in the preceding 24 h interval. We first briefly comment on the effect of plasmapause position for the ground-based events. For the 12 February 2004 event K_{pmax} was 5 corresponding to $L_{\mathrm{pp}} = 3.3$ (i.e. between NUR and TAR in Fig. 4a) and for the 6 March 2003 event K_{pmax} was 4+ corresponding to $L_{\mathrm{pp}} = 3.6$ (between HAN and NUR in Fig. 9a). The latitude-independent H component peak at 10 mHz between 15:00–15:20 UTC on 12 February 2004 and the peaks observed in the D component on 6 March 2003 are larger and/or sharper toward higher latitudes, even beyond the plasmapause. These features of the observed Pc3–4 waves are consistent with the spatial structure of a plasmaspheric virtual mode resonance (VMR) as modelled by Lee and Takahashi (2006). They found that resonant frequencies of the VMR observed in the radial (poloidal) component peak near the plasmapause. The VMR also extends beyond the plasmapause. Moreover, the radial component amplitudes are larger in the plasmatrough than deep in the plasmasphere.

The relationship between plasmapause position and the spectral structure of the events incorporating satellite data is more difficult to interpret. On 6 November 2003, the nominal plasmapause position $L_{\mathrm{pp}} = 4.1$, i.e. between SOD and HAN. The peak at 22 mHz, which we believe may be the signature of an FMR, was clearly observed in the CHAMP poloidal and compressional components, the latter with smaller amplitude. This peak was also observed at all MM100 stations with nearly equal amplitudes, thus this component seems to be hardly affected by the plasmapause. We believe that the peaks close to 30 mHz, where the CHAMP toroidal component has the largest amplitude, correspond to the UW activity (estimated $f_{\mathrm{UW}} = 27$ mHz).

The 16 March 2003 event was the most complex of the events presented. During the event L_{pp} was about 3.6, i.e. between HAN and NUR stations. The most intense peak at 24 mHz, which we ascribe to an FMR, had a clear minimum at HAN, NUR and TAR, i.e. at the plasmapause. This event was also clearly observable in the poloidal and compressional components of CHAMP. The 36 mHz peak, which is most likely related to UW activity, showed a similar structure at the ground stations; however, the corresponding peaks in CHAMP components are not significant. The observed features of these two components correspond to the FMR modelled by Allan et al. (1986a) with a node on the plasmapause. We also note that for this event the plasmapause seems to influence the spatial structure of other frequency components. The 51 mHz component was observed only outside the plasmapause, while the 62 mHz component, on the other hand, was observable only inside the plasmapause.

The radial component of a compressional mode is expected to be observed in the H component and not in the D component on the ground. Due to coupling, however, these waves can also appear in the D component. Actually, we found that the FMR related constant tones show up more clearly in the D component in most cases. In the H component the resonant structure is overwhelmed by the local field line resonances. That is why we used cross spectra computed from several stations to identify FMRs/VMRs in the H component.

In Sects. 3.1 and 3.2 we mentioned and briefly discussed the results of Samson et al. (1995) and Menk et al. (2000), who reported on the power spectra of ULF waves observed in magnetometer data recorded at low latitudes in the latitudinal range $1.3 < L < 2.0$. Their studies showed that the spectral bands of individual harmonics of the FLRs seen by ground-based magnetometers have envelopes that are typically 10's

of mHz wide, as seen in our spectra presented above. However, their spectra also exhibited a fine scale structure of multiple, closely spaced, spectral peaks with separations of about 3 to 5 mHz, which they ascribed to compressional cavity or waveguide modes. Samson et al. (1995) and Waters et al. (2000) developed models that could reproduce the important features of these low-latitude ULF wave power spectra in terms of the interaction between waveguide and field line resonance modes. The separations of spectral peaks that we observed in fast mode waves on CHAMP differed significantly from the above; the spacing typically observed in our dynamic spectra was approximately 20 mHz and roughly half this in averaged FFT spectra. We ascribe the smaller spacing in the averaged spectra to the intermittent nature and associated variable frequency of the signals. In order to determine whether we could observe fine structure in FLR peaks as reported by Samson et al. (1995) and Menk et al. (2000), we recomputed the FFT spectra for some of our events with greater spectral resolution, i.e. with no averaging of spectral estimates, in a manner similar to Menk et al. (2000). As was the case with the spectra presented by Menk et al. (2000), the most striking aspect of the spectra was the appearance of common peaks across stations and the narrow and consistent spacing between many of these peaks. However, it was also clear that the fine structure within the broader FLR peaks is not statistically significant. We also did tests to determine whether we could identify any fine structure in Pc3–4 pulsation spectra using MESA by increasing the PEF order in steps to the maximum possible value. We found that the main structures in the dynamic spectra remained essentially the same and there was no evidence of any fine structure. Consequently, we are obliged to assume that the fine structure reported by Samson et al. (1995) and Menk et al. (2000) is not real but rather an artefact of the parameters used in the data processing.

There have been a few other reports on observations of possible fast mode resonances, none of which mentioned finding any fine structure as reported by Samson et al. (1995) and Menk et al. (2000). Kim and Takahashi (1999) studied the properties of Pc3–4 pulsations on the dayside simultaneously observed in magnetic field data from the CCE satellite at $L = 2$–3 and at the Kakioka ground station ($L = 1.25$). They identified 63 cases of compressional fast mode waves in the frequency range of 20 ± 10 mHz, sometimes with higher frequency harmonics that were often accompanied by nearly identical magnetic pulsations at Kakioka. They were not able to definitively determine whether the fast mode waves were due to a plasmaspheric cavity mode, an evanescent mode, or a combination of types. Although Kim and Takahashi (1999) were able to demonstrate that compressional Pc3–4 pulsations exist in the low-L magnetosphere and that they give rise to pulsations on the ground, they concluded that further study was required to distinguish between the cavity and evanescent modes. Takahashi et al. (2009) reported a global pulsation event in which ground-based magnetometer arrays detected dayside magnetic pulsations at a common frequency of ~ 15 mHz at all locations below $L = 4$. The magnetic field measured by the GOES 8 geostationary satellite on the dayside showed no evidence of the peak at 15 mHz but indicated elevated broadband (7–80 mHz) ULF power in the compressional component. Takahashi et al. (2009) suggested that the global pulsations originated from a compressional MHD eigenmode oscillation, consistent with a virtual resonance in the inner magnetosphere (Lee and Kim, 1999), stimulated by the broadband external disturbance. Takahashi et al. (2010) made multipoint observations of a Pc4 pulsation event in the dayside plasmasphere. The primary data sources was the THEMIS-A satellite, which was moving outward from $L = 1.5$ to $L = 6.6$ near noon, and a number of low and midlatitude ground stations. On the satellite they detected radially standing fast mode waves characterised by oscillations in the azimuthal electric field and the radial and compressional magnetic field components. At the ground stations, Pc4 pulsations with nearly identical waveforms were observed at all locations with a spectral peak at 11 mHz. They interpreted the observations as convincing evidence of fast mode waves trapped in the dayside plasmasphere and found excellent agreement between their observations and theoretical models.

There have been suggestions that resonances in the Pc5 band at high latitudes can be driven by variations in solar wind dynamic pressure (Eriksson et al., 2006). Kepko et al. (2002) and Stephenson and Walker (2010) attributed multiharmonic Pc5 pulsations to forcing by periodic changes in solar wind dynamic pressure. To the best of our knowledge, there has not been any evidence to show that Pc3–4 pulsations are driven by these mechanisms. Clearly, more research is required to investigate the possible drivers of FMRs in the magnetosphere.

Waters et al. (2002) investigated experimental methods for the detection of ultralow-frequency cavity modes using spacecraft data. They suggested four methods for the detection of FMRs in satellite data. We applied the first two of these methods to show that signals with quasi-constant frequency often persist in the fast mode components as CHAMP rapidly traverses L shells and which we suggest are evidence of FMRs. However, a shortcoming of our endeavours to demonstrate the occurrence of FMRs is that we were unable to confirm that the fast mode waves were standing waves, which requires the application of the Waters et al. (2002) methods (3 and 4). Unfortunately, these could not be applied, since they require either dual satellites with magnetic field data or a single satellite with magnetic and electric field data, neither of which is applicable in CHAMP's case. We look forward to the Swarm mission, which will consist of three CHAMP-like satellites each with magnetic and electric field data, providing the opportunity to resolve the above question.

Acknowledgements. This work was partially funded by a grant from the Hungarian–South African Intergovernmental Science and Technology Cooperation Agreement and by a research grant from the National Research Foundation in South Africa.

Topical Editor I. A. Daglis thanks two anonymous referees for their help in evaluating this paper.

References

Allan, W., White, S. P., and Poulter, E. M.: Magnetospheric coupling of hydromagnetic waves – Initial results, Geophys. Res. Lett., 12, 287–290, 1985.

Allan, W., Poulter, E. M., and White, S. P.: Hydromagnetic wave coupling in the magnetosphere – Plasmapause effects on impulse-excited resonances, Planet. Space Sci., 34, 1189–1200, 1986a.

Allan, W., White, S. P., and Poulter, E. M.: Impulse-excited hydromagnetic cavity and field-line resonances in the magnetosphere, Planet. Space Sci., 34, 371–385, 1986b.

Baransky, L. N., Borovkov, J. E., Gokhberg, M. B., Krylov, S. M., and Troitskaya, V. A.: High resolution method of direct measurement of the magnetic field lines' eigenfrequencies, Planet. Space Sci., 33, 1369–1374, 1985.

Barnes, A.: Theory of Generation of Bow-shock-associated Hydromagnetic Waves in the Upstream Interplanetary Medium, Cosmic Electrodynamics, 1, 90–114, 1970.

Bendat, J. S. and Piersol, A. G.: Measurement and Analysis of Random Data, John Wiley & Sons, New York, 1966.

Bol'shakova, O. V. and Troitskaya, V. A.: Relation of the imf direction to the system of stable oscillations, Doklady Akademii Nauk (Proceedings of the Russian Academy of Sciences), 180, 343–346, 1968.

Carpenter, D. L. and Anderson, R. R.: An ISEE/whistler model of equatorial electron density in the magnetosphere, J. Geophys. Res., 97, 1097–1108, doi:10.1029/91JA01548, 1992.

Chen, W. Y. and Stegen, G. R.: Experiment with maximum entropy power spectra of sinusoids, J. Geophys. Res., 79, 3019–3022, 1974.

Clausen, L. B. N., Yeoman, T. K., Fear, R. C., Behlke, R., Lucek, E. A., and Engebretson, M. J.: First simultaneous measurements of waves generated at the bow shock in the solar wind, the magnetosphere and on the ground, Ann. Geophys., 27, 357–371, doi:10.5194/angeo-27-357-2009, 2009.

Engebretson, M. J., Zanetti, L. J., Potemra, T. A., and Acuna, M. H.: Harmonically structured ULF pulsations observed by the AMPTE CCE magnetic field experiment, Geophys. Res. Lett., 13, 905–908, 1986.

Engebretson, M. J., Zanetti, L. J., Potemra, T. A., Baumjohann, W., Lühr, H., and Acuna, M.H.: Simultaneous Observation of Pc3–4 Pulsations in the Solar Wind and in the Earth's Magnetosphere, J. Geophys. Res., 92, 10053–10062, 1987.

Eriksson, P. T. I., Blomberg, L. G., Schaefer, S., and Glassmeier, K.-H.: On the excitation of ULF waves by solar wind pressure enhancements, Ann. Geophys., 24, 3161–3172, doi:10.5194/angeo-24-3161-2006, 2006.

Fairfield, D. H.: Bow Shock Associated Waves Observed in the Far Upstream Interplanetary Medium, J. Geophys. Res., 74, 3541–3553, 1969.

Gary, S. P.: Electromagnetic Ion/Ion Instabilities and their Consequences in Space Plasmas: A Review, Space Sci. Rev., 56, 373–415, 1991.

Glassmeier, K.-H.: On the influence of ionospheres with non-uniform conductivity distribution on hydromagnetic waves, J. Geophys., 54, 125–137, 1984.

Heilig, B., Lühr, H., and Rother, M.: Comprehensive study of ULF upstream waves observed in the topside ionosphere by CHAMP and on the ground, Ann. Geophys., 25, 737–754, doi:10.5194/angeo-25-737-2007, 2007.

Heilig, B., Lotz, S., Verõ, J., Sutcliffe, P., Reda, J., Pajunpää, K., and Raita, T.: Empirically modelled Pc3 activity based on solar wind parameters, Ann. Geophys., 28, 1703–1722, doi:10.5194/angeo-28-1703-2010, 2010.

Heilig, B., Sutcliffe, P. R., Ndiitwani, D. C., and Collier, A. B.: Statistical study of geomagnetic field line resonances observed by CHAMP and on the ground, J. Geophys. Res., accepted, doi:10.1002/jgra.50215, 2013.

Jenkins, G. M. and Watts, D. G.: Spectral Analysis and its Applications, Holden-Day, San Francisco, 1968.

Kepko, L., Spence, H. E., and Singer, H. J.: ULF waves in the solar wind as direct drivers of magnetospheric pulsations, Geophys. Res. Lett., 29, 1197, doi:10.1029/2001GL014405, 2002.

Kim, K. H. and Takahashi, K.: Statistical analysis of compressional Pc3-4 pulsations observed by AMPTE CCE at $L = 2$–3 in the dayside magnetosphere, J. Geophys. Res., 104, 4539–4558, 1999.

Kivelson, M. G. and Southwood, D. J.: Resonant ULF waves: A new interpretation, Geophys. Res. Lett., 12, 49–52, 1985.

Le, G. and Russell, C. T.: A study of ULF wave foreshock morphology – II: spatial variation of ULF waves, Planet. Space Sci., 40, 1215–1225, 1992.

Le, G. and Russell, C. T.: The Morphology of ULF Waves in the Earth's Foreshock, in: Solar Wind Sources of Magnetospheric Ultra-Low-Frequency Waves, Geophys. Monogr. Ser., vol. 81, edited by: Engebretson, M. J., Takahashi, K., and Scholer, M., pp. 87–98, AGU, Washington, D.C., 1994.

Lee, D.-H. and Kim, K.: Compressional MHD waves in the magnetosphere: A new approach, J. Geophys. Res., 104, 12379–12385, 1999.

Lee, D.-H. and Takahashi, K.: MHD Eigenmodes in the Inner Magnetosphere, in: Magnetospheric ULF Waves: Synthesis and New Directions, edited by: Takahashi, K., Chi, P. J., Denton, R. E., and Lysak, R. L., Geophys. Monogr. Ser., vol. 169, AGU, Washington, D.C., doi:10.1029/GM169, 73–89, 2006.

Menk, F. W., Fraser, B. J., Waters, C. L., Ziesolleck, C. W. S., Feng, Q., Lee, S. H., and McNabb, P. W.: Ground Measurements of Low Latitude Magnetospheric Field Line Resonances, in: Solar Wind Sources of Magnetospheric Ultra-Low-Frequency Waves, Geophys. Monogr. Ser., vol. 81, edited by: Engebretson, M. J., Takahashi, K., and Scholer, M., pp. 299–310, AGU, Washington, D.C., 1994.

Menk, F. W., Waters, C. L., and Fraser, B. J.: Field line resonances and waveguide modes at low latitudes: 1. Observations, J. Geophys. Res., 105, 7747–7761, 2000.

Ndiitwani, D. C. and Sutcliffe, P. R.: The structure of low-latitude Pc3 pulsations observed by CHAMP and on the ground, Ann. Geophys., 27, 1267–1277, doi:10.5194/angeo-27-1267-2009, 2009.

Ndiitwani, D. C. and Sutcliffe, P. R.: A study of L-dependent Pc3 pulsations observed by low Earth orbiting CHAMP satellite, Ann. Geophys., 28, 407–414, doi:10.5194/angeo-28-407-2010, 2010.

Otnes, R. K. and Enochson, L.: Digital Time Series Analysis, John Wiley & Sons, New York, 1972.

Plaschke, F., Glassmeier, K.-H., Sibeck, D. G., Auster, H. U., Constantinescu, O. D., Angelopoulos, V., and Magnes, W.: Magnetopause surface oscillation frequencies at different solar wind conditions, Ann. Geophys., 27, 4521–4532, doi:10.5194/angeo-27-4521-2009, 2009.

Reigber, C., Lühr, H., and Schwintzer, P.: CHAMP mission status, Adv. Space Res., 30, 129–134, 2002.

Russell, C. T. and Hoppe, M. M.: The dependence of upstream wave periods on the interplanetary magnetic field, Geophys. Res. Lett., 8, 615–617, 1981.

Saito, T.: A new index of geomagnetic pulsation and its relation to solar M-regions, Ionosph. Space Res., 18, 260–274, 1964.

Samson, J. C., Harrold, B. G., Rouhoniemi, J. M., Greenwald, R. A., and Walker, A. D. M.: Field line resonances associated with MHD waveguides in the Earth's magnetosphere. Geophys. Res. Lett., 19, 441–444, 1992.

Samson, J. C., Waters, C. L., Menk, F. W., and Fraser, B. J.: Fine structure in the spectra of low latitude field line resonances, Geophys. Res. Lett., 22, 2111–2114, 1995.

Stephenson, J. A. E. and Walker, A. D. M.: Coherence between radar observations of magnetospheric field line resonances and discrete oscillations in the solar wind, Ann. Geophys., 28, 47–59, doi:10.5194/angeo-28-47-2010, 2010.

Sutcliffe, P. R. and Lühr, H.: A comparison of Pi2 pulsations observed by CHAMP in low Earth orbit and on the ground at low latitudes, Geophys. Res. Lett., 30, 2105, doi:10.1029/2003GL018270, 2003.

Takahashi, K., McPherron, R., and Terasawa, T.: Dependence of the spectrum of Pc 3-4 pulsations on the interplanetary magnetic field, J. Geophys. Res., 89, A5, doi:10.1029/JA089iA05p02770, 1984.

Takahashi, K., Berube, D., Lee, D.-H., Goldstein, J., Singer, H. J., Honary, F., and Moldwin, M. B.: Possible evidence of virtual resonance in the dayside magnetosphere, J. Geophys. Res., 114, A05206, doi:10.1029/2008JA013898, 2009.

Takahashi, K., Bonnell, J., Glassmeier, K.-H., Angelopoulos, V., Singer, H. J., Chi, P. J., Denton, R. E., Nishimura, Y., Lee, D.-H., Nosé, M., and Liu, W.: Multipoint observation of fast mode waves trapped in the dayside plasmasphere, J. Geophys. Res., 115, A12247, doi:10.1029/2010JA015956, 2010.

Tanaka, Y.-M., Yumoto, K., Shinohara, M., Kitamura, T.-I., Solovyev, S. I., Vershinin, E. F., Fraser, B. J., and Cole, D.: Coherent Pc 3 pulsations in the prenoon sector observed along the 210° magnetic meridian, Geophys. Res. Lett., 25, 3477–3480, 1998.

Troitskaya, V. A., Plyasova, T. A., and Gul'elmi, A. V.: Relationship between Pc2–4 pulsations and the interplanetary field. Doklady Akademii Nauk (Proceedings of the Russian Academy of Sciences), 197, 1312–1314, 1971.

Troitskaya, V. A.: Discoveries of sources of Pc2–4 waves – A Review of research in the former USSR, in: Solar Wind Sources of Magnetospheric Ultra-Low-Frequency Waves, Geophys. Monogr. Ser., vol. 81, edited by: Engebretson, M. J., Takahashi, K., and Scholer, M., pp. 45–54, AGU, Washington, D.C., 1994.

Tukey, J. W.: An introduction to the calculation of numerical spectrum analysis, in: Advanced Seminar on Spectral Analysis of Time Series, edited by: Harris, B., John Wiley & Sons, New York, 1967.

Vellante, M., Lühr, H., Zhang, T. L., Wesztergom, V., Villante, U., Lauretis, M. D., Piancatelli, A., Rother, M., Schwiegenschuh, K., Koren, W., and Magnes, W.: Ground/satellite signatures of field line resonance: A test of theoretical predictions, J. Geophys. Res., 109, A06210, doi:10.1029/2004JA010392, 2004.

Verõ, J. and Miletits, Cz.: Impulsive pulsation events and pulsation beats, J. Atmos. Terr. Phys., 56, 433–445, 1994.

Verõ, J., Lühr, H., Vellante, M., Best, I., Střeštik, J., Miletits, J. C., Holló, L., Szendrõi, J., and Zieger, B.: Upstream waves and field line resonances: simultaneous presence and alternation in Pc3 pulsation events, Ann. Geophys., 16, 34–48, doi:10.1007/s00585-997-0034-1, 1998.

Waters, C. L., Menk, F. W., and Fraser, B. J.: The resonance structure of low latitude Pc3 geomagnetic pulsations, Geophys. Res. Lett., 18, 2293–2296, 1991.

Waters, C. L., Menk, F. W., and Fraser, B. J.: Low-latitude geomagnetic field line resonance: experiment and modeling, J. Geophys. Res., 99, 17547–17558, 1994.

Waters, C. L., Harrold, B. G., Menk, F. W., Samson, J. C., and Fraser, B. J.: Field line resonances and waveguide modes at low latitudes, 2, A model, J. Geophys. Res., 105, 7763–7774, 2000.

Waters, C. L., Takahashi, K., Lee, D.-H., and Anderson, B. J.: Detection of ultralow-frequency cavity modes using spacecraft data, J. Geophys. Res., 107, 1284, doi:10.1029/2001JA000224, 2002.

Yumoto, K.: Low Frequency Upstream Waves as a Probable Source of Low Latitude Pc3–4 Magnetic Pulsations. Planet. Space Sci., 33, 239–249, 1985.

Yumoto, K., Saito, T., Tsurutani, B. T., Smith, E. J., and Akasofu, S. I.: Relationship between the IMF magnitude and Pc3 magnetic pulsations in the magnetosphere, J. Geophys. Res., 89, 9731–9740, 1984.